UNIVERSITY OF TARTU

FACULTY OF SCIENCE AND TECHNOLOGY

INSTITUTE OF ECOLOGY AND EARTH SCIENCES

DEPARTMENT OF GEOLOGY

Master thesis in Geology (30 EAP)

Magnetic anomaly model of the Lonar meteorite impact crater in Maharastra, India

Kalle Kiik

Supervisor: Jüri Plado

Allowed for defence:

Supervisor: ……..

Head of department: ……..

Tartu 2019

Abstract

Magnetic anomaly model of the Lonar meteorite impact crater in Maharastra, India

Lonar impact crater and its surrounding area was studied using a proton magnetometer and hand-held magnetic susceptibility meter. Based on these measurements an anomaly model of the crater was made. Motivation for the study came from a previous article which modelled only a small part of the crater centre as well as the general interest in understanding impact processes in basaltic rocks. Measurements show the crater has an anomaly which reaches 2600 nT positive to -2350 nT negative values at the rim. The crater floor has negative values of up to -1400 nT. Beyond the rim exists a relatively smooth magnetic field. Modelling shows that a large part of the anomaly is created by the highly magnetized target, the Deccan Traps. Breccia and crater lake sediments are homogeneous and less magnetized, in turn accounting for a lesser amount of the magnetic anomaly.

Keywords: Magnetic anomaly, modelling, Lonar impact crater, geophysics

CERCS code: P500 - Geophysics, physical oceanography, meteorology

Annotatsioon

Indias Maharastra osariigis asuva Lonar meteoriidikraatri magnetiline mudel

Lonar meteoriidikraatrit ja selle ümbritsevat ala uuriti prootonmagnetomeetri ja käeshoitava “kappameetriga”. Mõõdetud tulemuste alusel loodi kraatri magnetiline mudel. Käesoleva töö idee tuli varasemast artiklist, kus modelleeriti Lonari magnetväljast ainult väikest osa kraatri keskel. Lisaks juhtis töö teema valikut üldine huvi mõistmaks plahvatusstruktuure basaltsetes kivimites. Magnetvälja mõõtmistest järeldub, et kraatri magnetvälja anomaalia ulatub vallil 2600 nT positiivsetest kuni -2350 nT negatiivsete väärtusteni. Kraatri põhja iseloomustab kuni -1400 nT suurune negatiivne anomaalia. Kraatri vallist eemal on magnetväli sujuv ning vähemuutlik. Modelleerimisega avastati, et suure osa anomaaliast põhjustavad sihtmärgiks olevad kõrgelt magnetiseeritud Deccan Trapi basaldid. Bretša ja järvesetted on aga sihtmärgist nõrgemalt magnetiseeritud kehad, mis põhjustavad väiksema osa magnetilisest anomaaliast.

Märksõnad: Magnetanomaalia, potentsiaalse välja mudeldamine, Lonar meteoriidikraater, geofüüsika

CERCS kood: P500 – Geofüüsika, füüsikaline okeanograafia, meteoroloogia

Table of contents

Introduction

Circular Lonar structure (19°58′N, 76°31′E) is located in Maharashtra State, Buldana District, India (Figure 1). It is a Quaternary aged 1.88 km in diameter (D) simple impact crater formed into Deccan Trap basalts (Fredriksson et al. 1973). First thoughts of Lonar's genesis included volcanic explosion, caldera, and sink-hole (Wadia 1919). First thoughts of an impact origin can, however, be attributed to Gilbert (1896), who mentioned Lonar's similarity to Canyon Diablo (presently Meteor) Crater (though referring to their cryptovolcanic origin). Cotton (1952) thought volcanic hypotheses improbable, referring to the fact that no recent volcanics in India exist. A shallow bore-hole was made by Nandy and Deo in 1961, providing information about crushed rock occurring below the lake sediments. Based on the drillhole data and morphology, Lafond and Dietz (1964) pointed out several inconsistencies (absence of pyroclastics, young age, and the scale of the feature being too big for steam explosions) with prior explanations. Based on similarities with other impact craters, they thought an impact origin likely. Definitive proof of cosmic origin came in the 1970-s after extensive drilling, trenching, geophysical, and geochemical studies by the Geological Survey of India (GSI) (Fredriksson et al. 1973).

Lonar impact crater has been formed into basaltic rocks making it an important analogy for Lunar or Mars cratering processes on Earth and providing a fascinating source for impact studies. It is, however, not the only impact crater in basaltic rocks on Earth. There are complex craters, Logancha [65°31′N, 95°56′E; D = 20 km; age = 40±20 Ma (Masaitis 1999)] in Russia and Vista Alegre [25°57′S, 52°41′W; D = 9.5 km; age < 65 Ma or ~ 115 Ma (see Crosta and Vasconcelos 2013)], in Brazil. Lonar is, however, the easiest to access and most extensively studied so far.

At first, possible impact craters are usually identified from topographical indications. With the help of global satellite imagery, widely available, possible impact structures can be easily looked for and extents delineated in case of exposed features (rim, central uplift). When a possible crater is found, structural mapping in the area is done with emphasis put to finding impact related shatter cones, melted ejecta, spherules, breccia, upturned rocks at the possible rim, meteorite fragments, or planar deformation features in the area. Geochemical research of suspected impact rocks may also help prove the presence of an impact crater. Drilling is usually carried out to find and delineate the breccia layer below the crater floor. Many craters though, are not easily recognizable from topography or are buried below sediments or water.

Geophysics is a relatively cheap and effective tool to use in these cases as well as provide supplementary information to help characterize craters.

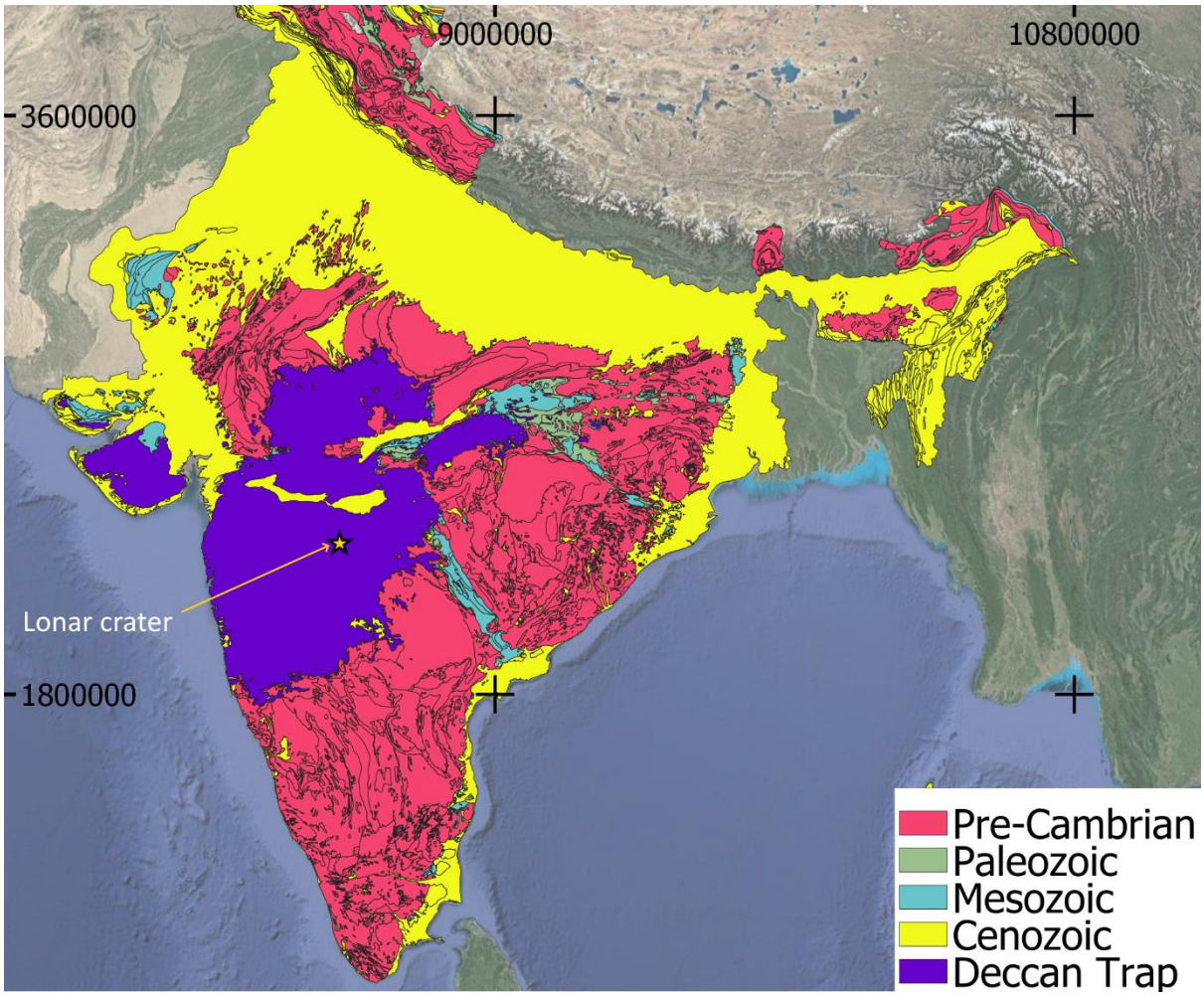

Figure 1. Generalized geological map of India. Purple shows the extent of Deccan Traps and yellow star shows the location of Lonar meteorite crater. Background map is a Google satellite image. Geological information is from: http://bhukosh.gsi.gov.in/Bhukosh/Public. Coordinates are in WGS 84/Pseudo-Mercator, EPSG:3857.

Thus, geophysical methods are extensively used in the study of terrestrial impact craters. Impact events subject the target to effects, which change its physical properties, making it distinguishable from the regional potential field. In this study, the magnetic method is applied. Magnetic anomalies related to impact cratering are complex, inherently from the complex nature of the magnetic properties of rocks. During an impact, several effects occur which can substantially alter the magnetic properties of rocks. These are mechanical, shock, thermal, and chemical effects. The mechanical effect comes from the brecciation of the rock. Rock gets smashed into pieces and moved. Due to this rock remanence directions are orientated randomly,

reducing the overall remanence strength of the brecciated rocks. Shock effects can remove existing remanent magnetization and remagnetize rocks in the direction of the prevailing magnetic field (Pressure (P) = 1 GPa; Hargraves and Perkins 1969), decrease magnetic susceptibility (*k*) (P = 10 GPa; Reznik et al. 2017) or produce/change magnetic minerals (P = 40 GPa, temperature (T) – 1000 °C; Chao 1968). Thermal effects prevail in the centre of impact where temperatures over the Curie temperatures of ferromagnetic minerals cause magnetic resetting and production of nonmagnetic glasses. Even at lower than Curie temperatures, minerals can obtain thermoremanent magnetization. Chemical effects through hydrothermal alteration might create new magnetic mineral phases, e.g., oxidation of magnetite to hematite (Pilkington and Grieve 1992).

Lonar is a perfect target to study the effects of small meteorite impact on the magnetic properties of rocks because of the homogeneous target basalts. Therefore, several studies are dedicated to rock magnetic properties of Lonar (Arif et al. 2012; Louzada et al. 2008; Rajasekhar and Mishra 2005; Rao and Bhalla 1984; Sangode et al. 2017; Weiss et al. 2010) with conflicting results yet to be resolved. There exists, however, only one surface-based geomagnetic survey (Rajasekhar and Mishra 2005), which attempts to model the magnetic anomaly within the crater. The present thesis aims to get a wider understanding of the magnetic anomaly caused by the impact process in basaltic rocks. To achieve this, the author performed (i) in situ measurements of *k* and (ii) magnetic modelling based on earlier measured magnetic field data.

1. Geological setting

1.1. Deccan Trap basalts – target rocks for Lonar impact

The Deccan Traps (The Deccan large igneous province) is a vast extrusion (Figure 1) of tholeiitic basaltic lava formed at the Cretaceous-Paleogene (K-Pg) boundary. Deccan volcanism took place over several million years from 69 to 62 Ma with periods of activity and inactivity (Chenet et al. 2007; Pande 2002), although exact duration and age estimates are contested by different authors. Basaltic lavas covered an area of 1 - 2.6 × 10^6 km^2 (Philpotts and Ague 2009) of which 500 000 km^2 remain nowadays after erosion (Vaidhyanadhan and Ramakrishnan 2008; Jay 2016). The maximum thickness of the traps is 1.8 km to 2.4 km whereas it is thicker in west and thinner in the east (Chenet et al. 2009; Harinarayana et al. 2007). In the Lonar area, thickness of the Deccan Trap is thought to be between 400 and 700 m (Fudali et al. 1980; Subbarao 1994, 1999). Volcanic stratigraphy for Deccan Traps is well developed in the western Mumbai region but is not well understood at the Lonar area (Subbarao

1999). Inside of Lonar crater, at the inner slope of rim, there are six 10 to 25 m thick outcropping basalt flows. Flows have an evolved internal stratigraphy with deeply weathered tops. Characteristic red paleosol has formed between flows due to the weathering in between the individual flows (Maloof et al. 2010).

1.2. Lonar Crater

MORPHOLOGY

The Lonar crater is near circular depression with an average diameter of 1.88 km and depth of ~135 m (Figure 2). The elevation at the base of the inner rim wall is 475 m a.s.l. and rim height is up to 600 m a.s.l., reaching 20-30 m over the surrounding rather flat plane. The bedrock in the rim dips radially apart from the crater centre at angles of 8-20° with some patches of overturned bedrock and characteristic for impact craters, stratigraphically inverted ejecta (Fredriksson et al. 1973; Fudali et al. 1980; Maloof et al. 2010; Nakamura et al. 2014). Because of ongoing erosion, the original crater could have had a rim crest diameter of 1.71 km with a rim height of 40-64 m (Fudali et al. 1980; Maloof et al. 2010).

Figure 2. View of Lonar crater from the southern watch tower.

A shallow saline/alkaline lake with depth up to 6 m occupies the middle part of the crater depression (Figures 2 and 3). The maximum depth of water column has fluctuated from 1.8 m (1953) to 6.8 m (2008) (Reddy et al. 2015). A deep gully, Dhar valley, with a perennial stream runs into the crater from the NE and has formed an alluvial fan that distorts the circularity of the lake. Apart from Dhar valley two seasonal and one perennial stream are also present. There are two different understandings about lake hydrology. Reddy et al. (2015) correlate the amount of rainfall as control of the hydrology with the groundwater flowing away from the crater. In this case, lake chemistry is regulated by rainfall and evaporation only. Komatsu et al. (2013), in contrast, say the gully, surface runoff, springs, and lithologically controlled groundwater contribute to the hydrology of the lake, also affecting the chemical composition of lake water.

Little Lonar

Situated 700 m north of Lonar crater is a small depression with a diameter of 300 m (Figure 2). It has been named "Little Lonar". It is hypothesised to also be of impact origin (Fredriksson et al. 1973; Fudali et al. 1980) but trenches dug by Maloof et al. (2010) uncovered 12.4 m of ejecta. From the bottom they found 4.8 m of ejecta without glass, then 2.8 m of glass-rich ejecta, 5.2 m of ejecta with no glass and the top 0.3 m to be colluvium. Due to ejecta emplacement times "Little Lonar" was ruled as a small natural depression with walls piled up by farmers.

Figure 3. Google Earth image of the Lonar crater area. Locations mentioned in the text are shown.

Age

Age of Lonar Crater is under dispute. Fission-track dating of shock-melted glass has dated the event to 50 ka (Fredriksson et al. 1973); unpublished radiocarbon dating of organic matter of the deep core samples provide a lower limit age to 15 and 30 ka (Sengupta and Bhandari 1988); thermoluminescence dating on impact glasses to 45, 52, or 67 ka (Sengupta et al.1997); radiocarbon measurements of histosols and organic-rich swamp mud to 11.65±0.7 ka (Maloof et al. 2010); $^{40}Ar/^{39}Ar$ measurements on 4 melt-rock samples to 570±47 ka (Jourdan et al. 2011); terrestrial in-situ cosmogenic nuclides (TCN) measurements of ^{10}Be and ^{26}Al to 37.5±5.0 ka (Nakamura et al. 2014).

IMPACTOR

The impactor of Lonar is thought to be a chondrite, based on Co, Cr, and Ni enrichment of impact spherules and due to the fact that no Fe-Ni fragments, phases, or other impactor fragments have not been found yet (Gupta et al. 2017; Misra et al. 2009). The size of the meteorite, using Pi-scaling relations (Melosh 1989), was estimated to be about 70, 86, or 120 m for iron, stony-iron, and ordinary chondrite, respectively (Chakrabarti and Basu 2006). Misra et al. (2010), based on ejecta concentration in the west and anisotropy of magnetic susceptibility, suggested fall of the Lonar projectile from the east at an angle of 30-45°.

INNER WALL STRUCTURE

Within the crater depression, a shallow borehole was drilled by Nandy and Deo (1961) to a depth of 91 m from the lake water level. After 5 m of water and 32 m of silty sediment, a zone of crushed rock (breccia) was encountered. Five additional boreholes (LNR-1 to LNR-5) have been drilled into the crater by the Geological Survey of India during field seasons 1971-1972 and 1978-1979 along SW-NE profile (Figure 4). Depths of drillholes: LNR-1 (310 m); LNR-2 (351 m); LNR-3 (310 m); LNR-4 (310 m); LNR-5 (400.25 m). Four drillholes were done on the lake with depth measured from the drilling barge and one, LNR-4, on the shore. For LNR-1 to LNR-4 the sediments were drilled with a rock roller bit thus no sediment core for these are available. Below it, common core drilling was done but the core recovery was low. At LNR-5 different equipment was used, and core drilling was done for sediments as well. Core recovery was improved but the breccia recovered was weakly consolidated powder with occasional basaltic fragments.

Based on drilling results, a post-impact sediment lens with a thickness of 100 m occurs is in the centre of the crater. The sediment lens consists of silt and unsorted basaltic sand. Below sediments, the breccia lens occurs, which consists of alternating patches of coarse breccia (rock fragments of meters to tens of meters in size) and microbreccia/basaltic powder (fragments of few centimeters to submicroscopic in size). Coarse breccia fragments show low or no shock metamorphism, whereas microbreccia exhibits moderate to strong shock metamorphism (Fredriksson et al. 1973). The breccia lens is described by Fredriksson et al. (1973) as disorganized: coarse breccia clasts are separated from each other by up to tens of meters sized patches of microbreccia. The exact extent of the brecciated zone is unknown, but it is > 225 m thick and limited to bottom 500-600 m below the crater floor (unpublished work by S.S. Rao

as cited in Maloof et al. 2010; Rajasekhar and Mishra 2005). Volume of the lens is calculated to be about 0.23 km^3 (Grieve et al. 1989).

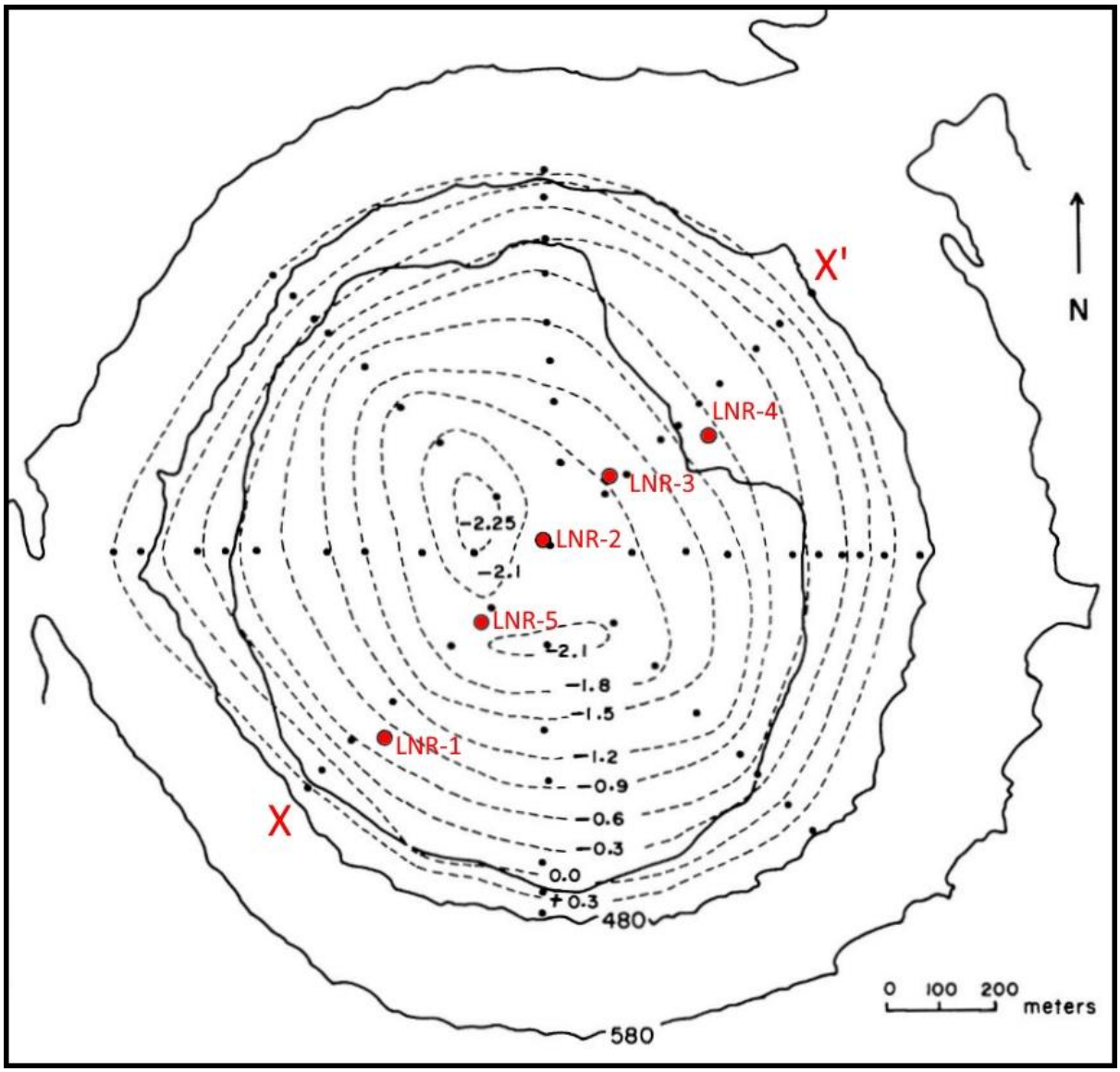

Figure 4. Gravity anomaly over the Lonar crater floor shown by dashed line contours. Black and red dots indicate locations of gravity stations and drillholes, respectively. X-X' is the magnetic anomaly profile by Rajasekhar and Mishra (2005). Modified after Fudali et al. (1980).

Initially, it was thought that all boreholes penetrated the allochthonous breccia lens, but a later interpretation by Fudali et al. (1980) showed that four (LNR-1 to LNR-4) of them did not reach the true bottom. LNR-5, the deepest borehole, bottomed in basaltic powder but the definitive delineation of breccia and the true crater bottom was thought to be impossible even for this drillhole. Below the true bottom, the basalts will also be fractured. This makes the pinpointing

of the separating boundary between the breccia and fractured rock very difficult, based solely on borehole data.

EJECTA LAYER

Ejected by the impact material surrounds the crater as an uninterrupted layer which spreads to an average distance of 1350 m from the rim. Past this distance, the ejecta blanket becomes patchy. The ejecta layer shows little to no erosional features thus originally the continuous ejecta layer must have reached only slightly bigger distances (1410 m in average; Fudali et al. 1980). The layer has recently been cultivated by farmers, but the effect seems to be minimal still (Figure 5). From the rim, the ejecta slopes at a small angle of 2-6°. Fudali et al. (1980) argued that the ejecta emplacement was a result of ballistic, but also fluidization components. It is because the ballistic model alone does not explain the distance of the ejecta, which should be attributed to ground hugging surges.

Figure 5. View away from the crater rim at the southern watchtower.

Fredriksson et al. (1973) divided the ejecta into two types: (i) lower, poorly stratified clasts and blocks, which show no evidence of shock and (ii) upper, ~1 m thick layer that contains little to intensely shocked clasts, patches of impact glass, as well as spherules. The uppermost shocked ejecta blanket was found by Fredriksson et al. (1973) to extend ~600 m continuously apart from the crater rim with shock pressure estimates for this ejecta reaching 60 GPa.

PREVIOUS GEOPHYSICAL RESEARCH AT LONAR CRATER

Gravity, magnetic, and seismic investigations have been carried out at Lonar crater in February 1964 by the GSI (Kailasam et al. 1964). This unpublished report is, however, inaccessible and results were found to be described in a report by Dube and Gupta (1978). Further gravity work was done in November 1977 (Fudali et al. 1980). Based on those gravity and magnetic data, as well as Subrahmanyam (1985) and Fudali and Subrahmanyam (1983), a geophysical model of crater interior was produced by Rajasekhar and Mishra (2005) (Figure 6).

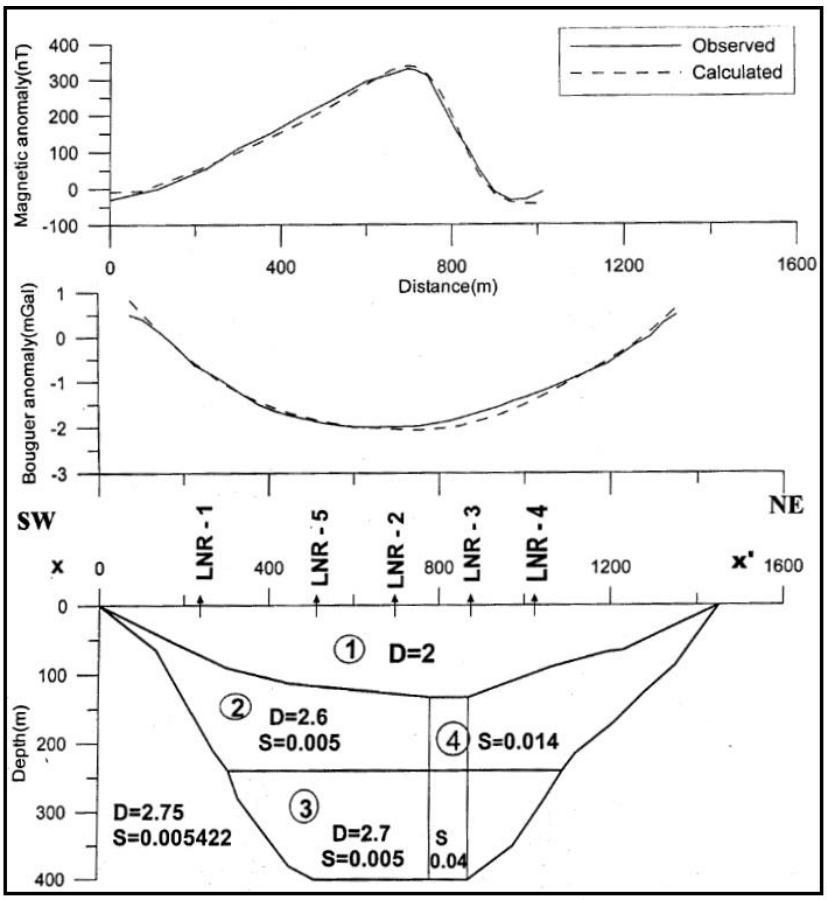

Figure 6. Magnetic (upper) and gravity (middle) anomalies of profile X-X' (for location see Figure 3). Lowermost is the model constructed to characterize the anomalies. The figure is after Rajasekhar and Mishra (2005).

Gravity measurements by Kailasam et al. (1964) were done around the crater lake at 8 stations and indicated the presence of a negative anomaly. These measurements were limited to the lake shore due to gravity meter not being suited for use on a boat. Additional work was carried out by the GSI in an alternate field season, using 36 underwater (made using LaCoste and Romberg model H underwater meter, which was lowered to the lake floor from a barge) and 76 land stations (made using Scintrex Prospecting Model CG-2). All water stations and some of the ground stations locations are shown in Figure 4. Water station locations were determined by triangulation from the shore and land station locations with plane table plus alidade survey (Fudali et al. 1980). Measurements of Kailasam et al. (1964) were combined with those by Fudali et al. (1980). Fudali et al. (1980) observed a gravity anomaly of ~ 3.6 mGal in amplitude, with a negative 2.25 mGal at the crater centre and a positive anomaly of ~1.4 at the rim. Generally, the anomaly is circular, but the interpreted isolines are slightly elliptical in the very central part with longer axis oriented NW-SE. North-west and south-east of the gravity contour centre are gravity lows, which were interpreted as thicker parts of the sedimentary lens. North-western gravity low was estimated as 115 m thick and south-eastern as 105 m. Model by Rajasekhar and Mishra (2005) shows a bowl shaped gravity anomaly with an amplitude of 2.5 mGal (Figure 6).

Total magnetic intensity (TMI) measurements were carried out by Kailasam et al. (1964). These were made along eight radial lines from the crater lake and upon the lake surface along seven N-S traverses. On the lake, a uniform TMI gradient of 1000 nT/km was acquired in the N-S direction, explained by the sub-trap topography and the Deccan Trap remanent magnetization. At that time definitive proof for the impact origin was not available, which probably lead to a completely non-impact related interpretation such as this. Also, the above authors noted values of 1500 - 2000 nT away from the crater, 4000 nT across the rim and 1500 - 2000 nT at the foot of the inner rim wall.

Rajasekhar and Mishra (2005) described a vertical component magnetic anomaly of 550 nT in amplitude over the crater floor. Their data were taken from previous magnetic field vertical component measurements done by Subrahmanyam (1985). They show a magnetic anomaly profile (Figure 4) from the lakeside only. The profile shows anomalous values of -30 nT at the shoreline in SW side of the Lonar lake. The values increase toward the centre of the lake till a maximum of 340 nT at the crater centre. Then, the values decrease rapidly back to zero (Figure 6).

A seismic study was carried out by Kailasam et al. (1964). Sounding was done in the lake as well as NE, E, and W at the lakeside in the crater floor. Two distinct layers were seen overlying the hard trap. Top layer with P-wave velocity of 1554 m/s, interpreted as a highly weathered silt-cumulative or decomposed trap rock, with a NE lakeside thickness of 25 m which reaches 76 m at crater centre. Middle layer with P-wave velocity of 2134 m/s, interpreted as less weathered trap rock or a crushed breccia zone, with a thickness of 67 m at the western sounding points to 100 m near the crater centre. According to seismic studies, the bottom hard trap floor varies from 91 m at NE to 183 m at the lake centre. With data from shot points not completely available, drawing seismic profiling across the crater was impossible and bedrock position not pinned down.

SHOCK PRESSURES AND TEMPERATURE OF IMPACT

Shock pressure estimates split into two for Lonar crater. First, it is suggested the shock pressure at the rim was about 3 GPa as based on experimental measurements by Nishioka and Funaki (2008). The pressure is thought to be enough to reorientate magnetic fabric and influence/distort the natural remanent magnetization (NRM) components, anisotropy of magnetic susceptibility as well as reduce k and magnetic remanence. It is thought the high coercivity/high temperature (HC/HT) component of the original Deccan Trap was affected by shock. Low coercivity/low temperature (LC/LT) component is roughly present-day field orientated and carries shock remanent magnetization (SRM) (Arif et al. 2012; Misra et al. 2010; Rao and Bhalla 1984).

Second set of studies imply the shock pressures to be low. At the crater rim area, pressures are thought to be about 0.2 - 0.5 GPa by Agarwal et al. (2016) and a numerical model by Louzada

An impact event can be separated into three stages: (i) contact and compression, (ii) excavation, and (iii) modification. All these stages show a different part of the same process, so, during impact one stage change into another gradually (Melosh 2004).

During contact and compression, contact is made with the target objects surface, transferring energy into the rocks below. The amount of energy is huge for a body travelling at several to tens of km/s. The contact generates strong shockwaves in both the impactor and target, and compressing them. The target is pushed downward and outward. When the shock wave reaches the top of the impactor, pressure is released with the impactor expansion upward. When this wave of pressure release reaches the impactor/target surface, the contact and compression stage has ended. The initial compression generates pressures of up to hundreds of GPa, liquefying or vaporizing the impactor. Excavation stage is characterized by the expansion of the shock pressure wave and its weakening into an elastic wave. The weakening is due to the energy loss by the shock wave expansion over an increasing hemispherical area and loss of the energy to heating the target. The high pressure exists only at the boundary of the shock wave; behind it, decompression occurs rapidly. These pressures can melt or vaporize rock at the high pressure parts or produce high pressure variants of minerals. Lower pressures might create fracturing, planar deformation or shatter coning. As the shock wave dissipates, the material acquires about 1/5 of the shock wave velocity which will then excavate the crater. Modification refers to the motion of the debris inside the crater. Movement up and away from the crater centre stops and reverses. This is thought to be due to gravity. Debris slides or drains back creating crater floor rise, central uplift, rim sinking or stepped terraces (Melosh 2004).

et al. (2008) confirming it with pressures less than 1 GPa reaching the rim. The same numerical model presents peak shock temperatures of above 200°C restricted to directly below the crater floor. These two studies, as well as Sangode et al. (2017), indicate no influence of impact-induced shock on the HC/HT component of NRM and argue the LC/LT component to be affected by viscous (VRM) and/or chemical remanent magnetization (CRM). Shock remanent magnetization was either not acquired by the rocks in the first place or overwritten by the VRM and/or CRM.

2. Sampling and methods

2.1. Magnetic field intensity measurements

Ground magnetic measurements were carried out in October 2017 by using two proton precession magnetometers G-856 (Geometrics). The magnetometers were carried by two people team, one person equipped with a magnetometer and another with a hand-held GPS device. Field-team included students and professionals from the Central University of Karnataka, India (Prof. Muddaramaiah Lingadevaru and Phd. student Hamim Jeelani Syed), University of Tartu, Estonia (PhD. Jüri Plado) and Adam Mickiewicz University, Poland (PhD. student Mateusz Szyszka). The land survey was conducted along variously oriented tracks by taking readings at approximately every 35 m. Additional measurements were done at the Lonar Lake, where the magnetometer and the team were carried by rubber rowing boat. Altogether area of 36 km^2 was covered (Figure 7).

Measurements that were made during nine running days, were corrected against diurnal variations. For corrections, a base station was established at the eastern rim of the crater. Also, magnetic observatory data by World Data Centre for Geomagnetism, Mumbai (http://wdciig.res.in/WebUI/Home.aspx; 18°53'36"N, 72°48'54"E) were applied. Amplitude of diurnal variations was up to 50 nT. Author of the thesis was supplied by corrected against diurnal variations magnetic data of the region. The corrections were done by Jüri Plado.

Figure 7. Locations of total magnetic intensity measurements at Lonar crater and its nearest surroundings; marked as red dots. Background is a Google satellite image. Coordinates are in WGS 84/Pseudo-Mercator, EPSG:3857.

2.2. Magnetic susceptibility measurements

In December 2018, author of the present thesis, with students from the Central University of Karnataka, India (PhD. students Hamim Jeelani Syed and Sharat Raj B.), carried out *in situ* magnetic susceptibility measurements with magnetic susceptibility meter SM-30 (ZH Instruments). The instrument has a 50 mm pick up coil which works at a frequency of 8 kHz. This allows for a resolution of 10^{-7} SI whereas most (68.81%) of the signal is generated within the topmost 1 cm of the rock/sediment (ZH Instruments 2009)

SM-30 can be operated in 6 different modes. In the present study, the interpolation mode, which includes three measurements [(i) free air, (ii) rock/sediment, and (iii) free air], was used. Using interpolation mode, a single measurement takes about 10 seconds and is automatically corrected against possible thermal drift. Acquired values represent apparent susceptibility because they cannot be normalized against mass or volume during outcrop measurements. Measured values, lithology, and GPS coordinates (taken from a mobile phone) were written into a field notebook. The data from the notebook was written into an MS Excel file, where it was systematized.

A total of 203 unique measurements were made. Magnetic susceptibility measurements (Figure 8) were carried out on the inner slopes of the Lonar crater, sediments around the crater lake and ejecta at Kinhi as well as Kalapani Dam sections (Figures 3 and 8). Rim traverses were done along four established pathways by people. Distance between individual measurements depended on the in-situ outcropping and the degree of basalt weathering. Values were taken from basalts and paleosols whenever a suitable in situ location was found. For lake sediments, the closest possible location to the current water level was taken after which a shovel was used to dig out the uppermost layer of dried out sediment to provide a flat surface for measurements.

Magnetic susceptibility (k) is considered the fundamental rock parameter in regard to magnetic exploration. The magnetic susceptibility is a measure of the amount to which a material can be magnetized. When a material is placed into an external magnetic field (H), a reorientation of atoms occurs, and their electron spins are aligned by the external field. This creates an induced magnetization (M) inside the material.

Magnetic susceptibility is expressed as a ratio of induced magnetization to external/applied magnetic field:

$$M=kH \rightarrow k=MH$$

H and M are measured in ampere/meter (A/m), which makes k a dimensionless unit. The k may be normalised against mass or molar mass.

All minerals/materials can be characterized by their behaviour in an external magnetic field. If a rock or material containing the mineral is in an external magnetic field, the body acquires a magnetization with an intensity proportional to the overall k of the body.

Minerals are divided into 3 groups (diamagnetic, paramagnetic, ferromagnetic) based on their behavior in the external magnetic field. Diamagnetic minerals have atoms with orbital electrons paired and get oriented to oppose the external field when one is applied, creating a net negative susceptibility. This occurs in minerals where the net magnetic moment of the atoms is zero when the external magnetic field is zero. Behaviour like this is usual for atoms which have a full electron shell and for minerals such as graphite, quartz, salt, and calcite. Diamagnetic minerals have k values of about -10^{-6} SI units. Paramagnetic minerals have a magnetic moment which is not zero in the absence of an external field. It occurs when one or more electron orbitals is unpaired. Magnetism parallel to an external field is acquired and magnetic moments are partially aligned with the external field. Most materials are paramagnetic. Paramagnetic minerals have a weak positive susceptibility of $+10^{-4}$. Metallic minerals rich in iron, nickel, cobalt have atomic magnetic moments which strongly align in large areas of the mineral, called magnetic domains. This is called ferromagnetism. It appears in materials which have atoms with unpaired electrons. These substances can generate a state of permanent magnetization independent of the external field. (Lowrie and Sheriff 2007).

Magnetic susceptibility is the reflection of mineral assemblage that forms a rock. Therefore, it is the most significant property to characterize geomagnetically anomalous bodies.

At Kinhi and Kalapani Dam sections profiles were made with measurements taken every 10 cm.

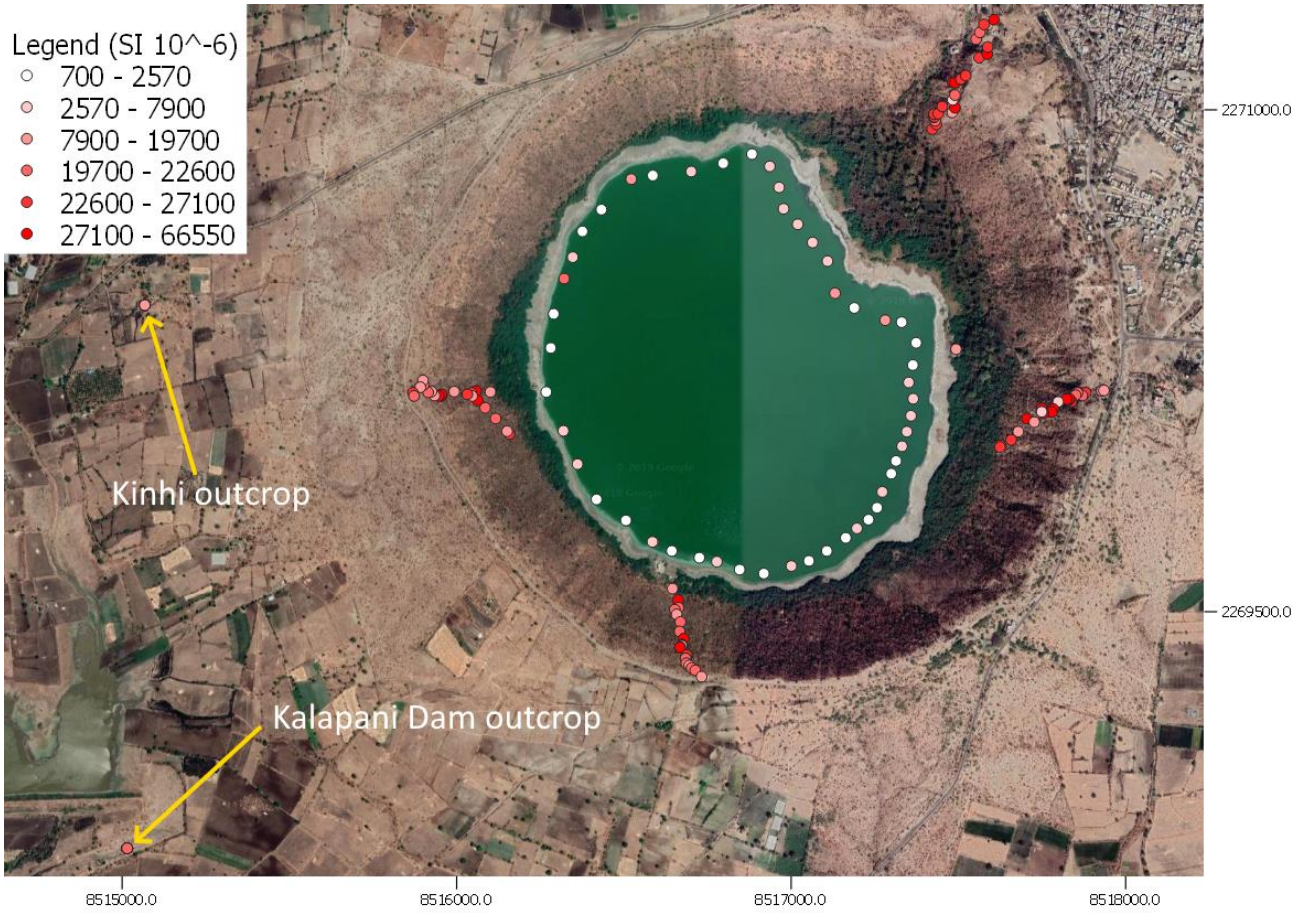

Figure 8. Locations and values of magnetic susceptibility at Lonar crater and ejecta outcrops. Background represents a Google satellite image (2019). Measurements appear within a lake because of changes in water level. Coordinates are in WGS 84/Pseudo-Mercator, EPSG:3857.

2.3. Magnetic anomaly modelling

There are several parameters which affect the magnetic field associated with a meteorite impact crater. Magnetic anomaly configuration depends on the contrast of *k* in rocks, depth, and orientation of the anomalous body, shape and size, remanent intensity values as well as the inducing magnetic field of the Earth. Forward modelling is the standard technique used in geophysics to describe anomalies, including magnetic anomalies.

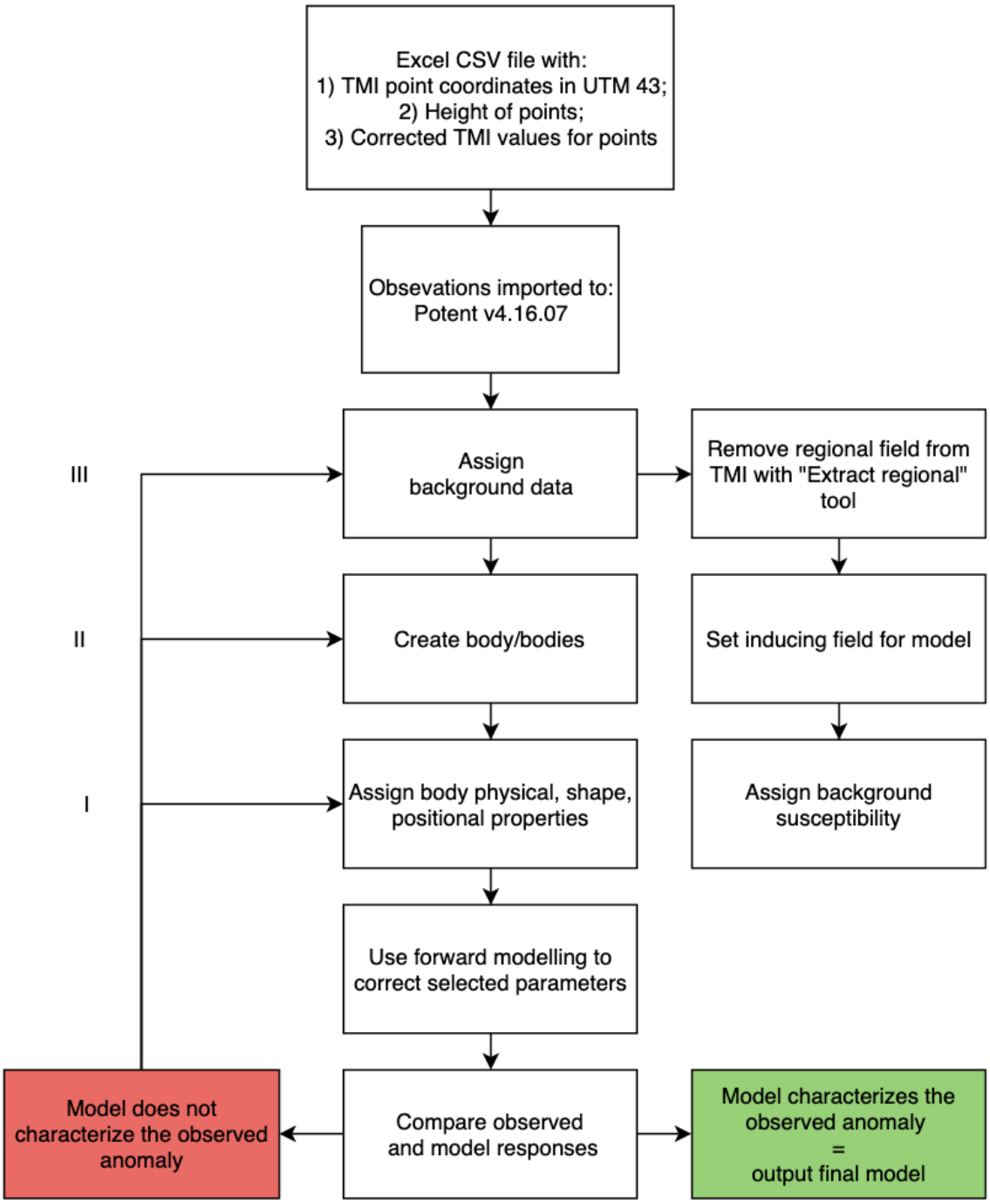

Figure 9. Workflow chart of the modelling process.

Software Potent v4.16.07, made by Geophysical Software Solutions, was used in forward modelling of the Lonar crater anomaly. It allows a 3D model, using simple geometrical shapes (ellipsoid, rectangle, cylinder, etc.) or a 2.5D stratigraphical model to be produced. The forward modelling workflow process is shown in Figure 9.

After importing data into Potent, the modelling was carried out as follows:

- Regional field elimination: the regional field needs to be subtracted from TMI values to be able to work with only the anomaly. In Potent "Extract regional" tool is used.
- Inducing field: An inducing field is applied according to the location, year and height of the measurements taken. The inducing field is calculated from the International Geomagnetic Reference Field (IGRF). The calculator is provided in the software.
- Background susceptibility: Background susceptibility is entered to account for the magnetic effects of surrounding rock.
- A body or several bodies from a variety of shapes is created.
- The body shape, size and magnetic parameters are modified to fit measured or expected values.
- Body parameters are inverted, changed automatically by the program or manually, to generate the same anomaly as field measurements indicate.
- If the model and observed responses are similar enough, the modelling process is complete. If they are not similar, relevant parameters (MS, remanent intensity, body size, etc.) are changed until observed and model responses match.

3. RESULTS

3.1. Total magnetic intensity measurements

The total magnetic intensity map (Figure 10) of the Lonar crater depicts a circular impact crater structure with highest (46038 nT) and lowest (41143 nT) TMI values in the area confined to the crater rim proximity. Beyond the crater rim is a relatively uniform magnetic field with a few short wavelength anomalies based on a small number of measurement points. These anomalies are randomly arranged with maximum values of -1000 to 1000 nT from the mean. Coinciding with Lonar town a positive anomaly of up to 1000 nT is seen but aside from it anomalies cannot be attributed to a specific feature. The anomalies appear to be natural magnetic field variations of the Deccan Traps.

In order to get the area anomaly map (Figure 11), the regional field was removed using the Potent software's *Regional* tool. With *Regional* tool control points are selected on the observed field map and coefficients (regional field) estimated as root-mean-square of the selected control points. The 75 control points were picked from outside the crater area (Appendix 1) and a uniform regional field of 43662.3 nT was estimated. The estimated regional field is subtracted from the TMI measurements and a residual field (anomaly map) is obtained.

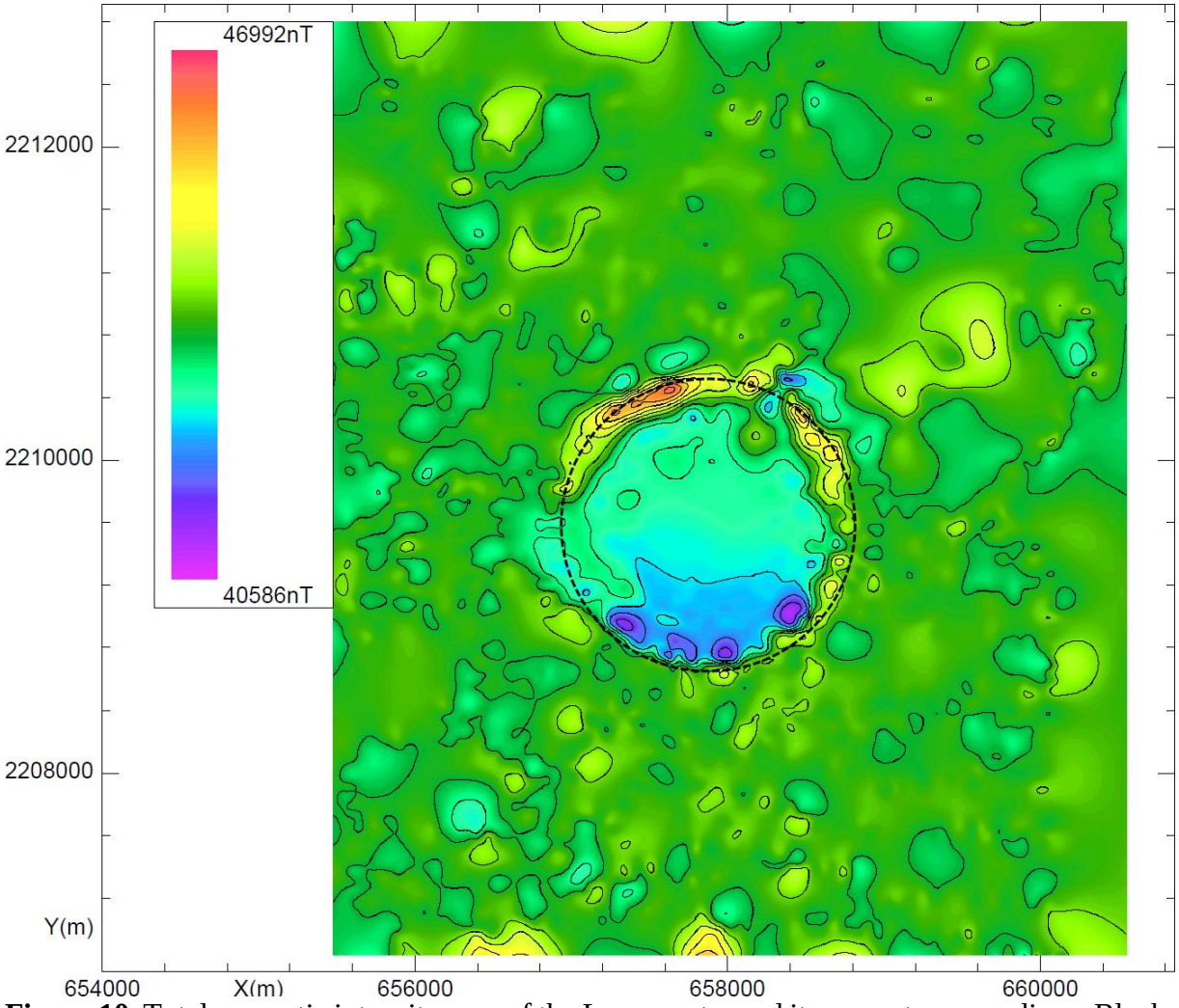

Figure 10. Total magnetic intensity map of the Lonar crater and its nearest surroundings. Black dotted line depicts the crater rim edge. Contour interval is 500 nT and coordinates are in UTM 43.

RESIDUAL (ANOMALY) MAP

Residual map of the Lonar impact crater is characterized by a circular magnetic anomaly which coincides with the morphology of the crater as illustrated by Figure 10. Distinct is the rim and crater floor. The rim has high positive values in the north and east of up to 2600 nT. These values, however, are not continuously positive from northern rim across to the eastern part of the rim. North-eastern part of the rim has high negative values of up to -1650 nT which coincides with the Dhar valley. Southern and western rim have high negative values of up to -2350 nT. Away from the crater rim, the anomaly disappears almost immediately.

Across the inner rim toward the crater floor northern and eastern positive values, of up to 2600 nT, turn rapidly negative, up to -1400 nT. At the southern and western inner rim, negative values decrease from -2350 nT to -1400 nT at the edge of the crater floor. On the crater floor,

negative values of -400 to -1400 nT are observed with a small slightly positive patch (200 nT) in the NE being the alluvial fan of the Dhar valley. A general decrease is seen in the negative values from the southern crater floor, with negative values of -1400 nT, to the northern lake shore with TMI of -400 nT. This gradient (~1000 nT/km) is similar to the magnetic field measured across the lake by Kalisam et al. (1964) of 1600 nT/mile or ~1000 nT/km.

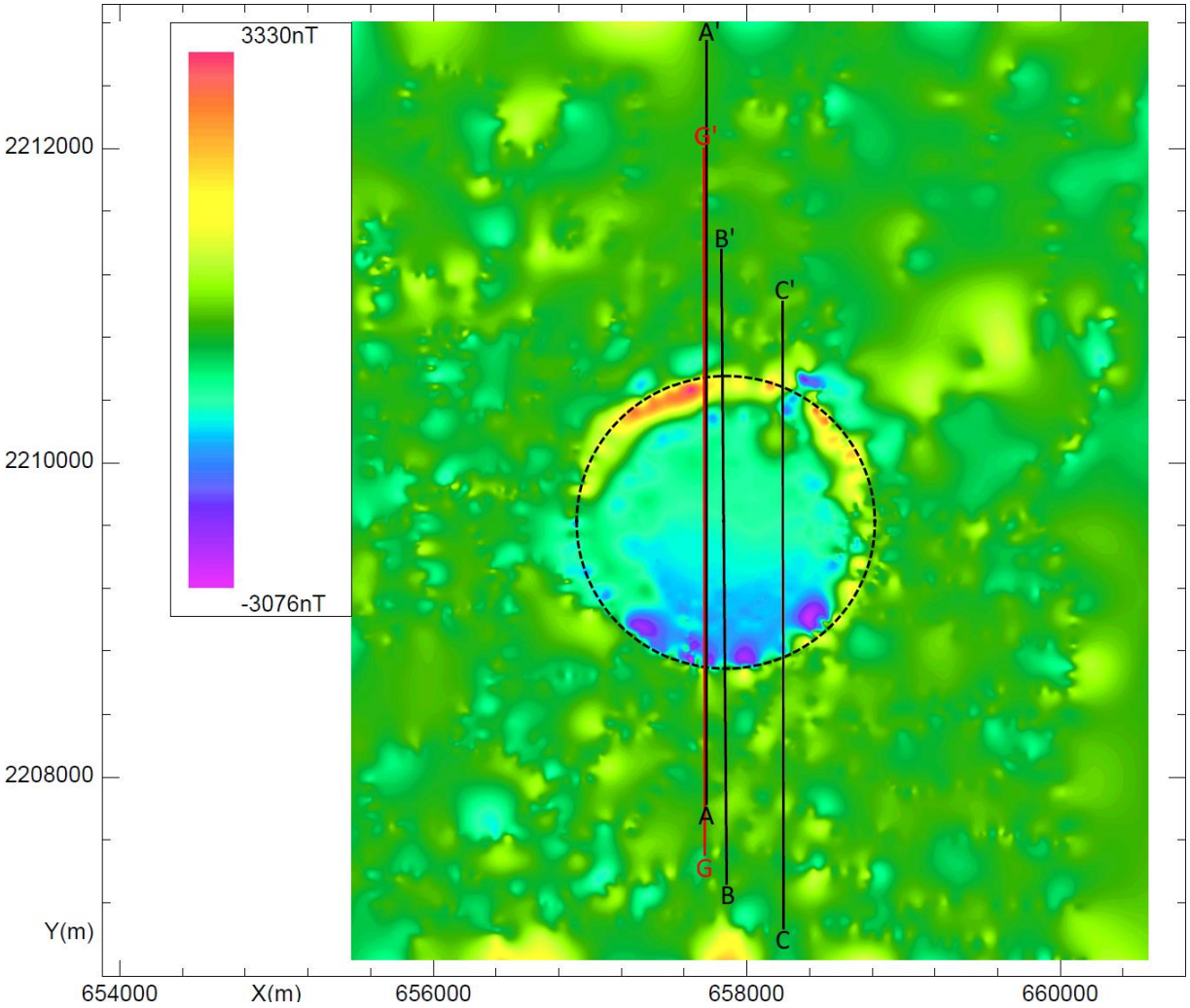

Figure 11. Residual magnetic field map of the Lonar crater. The dotted line depicts the crater rim edge. A-A', B-B' and C-C' are the magnetic anomaly cross-sections shown in Figures 13, 14 and 15 and G-G' the gravity anomaly cross-section in Figure 16. Coordinates are in UTM 43.

3.2. Magnetic susceptibility

Four *k* traverses were made while ascending or descending along the crater inner slope in north-eastern, eastern, southern, and western sides (Figure 8). In the walls flows of basalt outcrop with layers of paleosol in between. The Deccan basalts have an average *k* value of 24000 × 10^{-}

^{6}SI and paleosols an average value of 6110·10^{-6}SI (Table 1). The basalt flows show relatively consistent values between 20000 and 25000·10^{-6}SI apart from one. This is a middle (altogether 3 flows were found in the eastern traverse) flow of the eastern traverse, that has an average value of 43710·10^{-6}SI. Histogram for all *k* measurements is shown in Figure 12. The distribution of basalts is unimodal with a slight positive skew. Measurements done on paleosols are too few to analyse the distribution.

Lake sediments consist of grey, brown or black silt and black basaltic sand (Figure 13). Silt of different colours comes first, under which black sand was sometimes encountered (depended on the digging depth). Silt sediments have average *k* values of 3099 × 10^{-6}SI. The black basaltic sand has *k* values of 10000 - 21000 × 10^{-6}SI. Distribution of lake sediments on the histogram (Figure 12) is asymmetrical with a strong positive skew. This depicts the dual nature of sediments well.

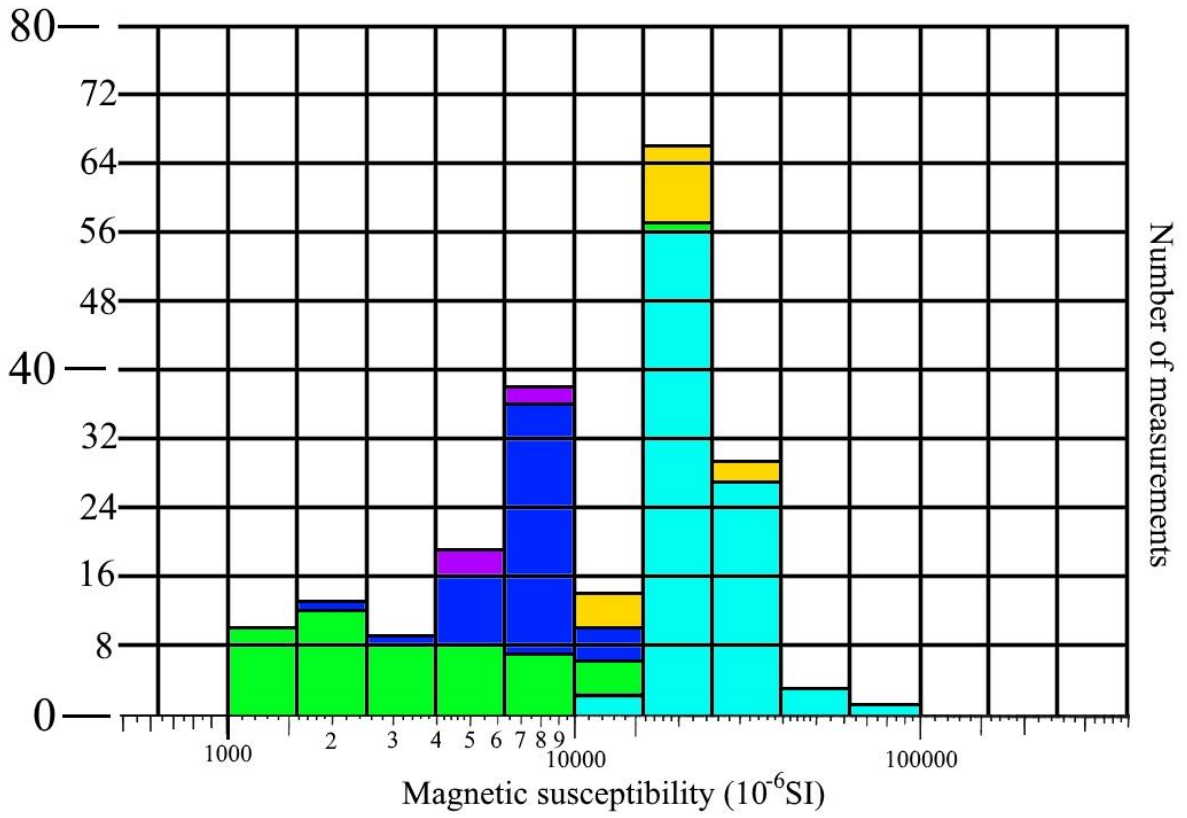

Figure 13. Histogram of magnetic susceptibility for lake sediments (green; n = 51), ejecta (blue; n = 43), paleosols between lava flows (purple; n = 5), basalt boulders in ejecta (yellow; n = 15) and basalts (light blue; n = 89). A total number of *k* measurements is 203.

Figure 13. Left picture shows magnetic susceptibility measurements taken on basalts. Picture on the right depicts lake sediments (From the top: (i) grey, (ii) brown and (iii) black silt). Bottom picture is of ejecta at Kinhi outcrop.

Ejecta at Kinhi (Figure 13) and Kalapani Dam has average *k* values of 7865 × 10^{-6}SI and 7010 × 10^{-6}SI, respectively. These values are similar to those measured in paleosols. Basalt boulders within ejecta exhibit values typical for basalts in the crater inner wall: 24400 × 10^{-6}SI in Kinhi

and 19414 × 10^{-6}SI in Kalapani Dam outcrops. Distribution of ejecta on the histogram (Figure 11) is unimodal with a negative skew. Basalt boulders within ejecta match the distribution of flow basalts.

Magnetic susceptibility measurements carried out on Deccan basalts in the course of this study are comparable to values found in the literature (Table 1).

Table 1. Magnetic susceptibility of Deccan Traps and Lonar crater by different authors and the present study.

	Magnetic susceptibility (10^{-6}SI)				Koenigsberger ratio (-)
	Average	Minimum	Maximum	Standard deviation	
		Deccan Traps			
Lonar lake (Rao and Bhalla 1984)	26000	17000	40200	7200	2.5 – 10.1 Average 5.93
Saurashtra (Chandrasekhar et al. 2002)	55000	14500	77500		0.15 – 2.02
Dhar region (Rao and Bhalla 1981)	43800	15700	72000		2.35 – 9.81
Lonar lake (Agarwal 2016)	39500	26000	55800	15200	
		Present study			
Lonar basalts	24000	11200	65500	9532	
Lonar lake silt sediments	3099	700	7900	2100	
Lonar paleosols	6110	4930	9330	2470	
Kinchi outcrop					
ejecta	7865	3560	11400	2141	
basalt boulders			24400		
Kalapani dam outcrop					
ejecta	7010	2390	8820	1425	
basalt boulders	19414	12400	30500	4970	

3.3. Modelling results

Magnetic anomaly modelling software, such as Potent, allow only *k* to be set as a background property. This is inadequate in the case of Lonar crater, where background basalts, in addition to *k*, have high remanent magnetization (several times higher than the inducing field) and well-known remanence directions (Table 2). For this reason, the Deccan Trap was modelled as a separate body acting as a background for the Lonar magnetic anomaly model. This allows profiling in only one direction and S – N was chosen. One gravity cross-section was also made to compare with previous gravity measurements (Fudali et al. 1980; Rajasekhar and Mishra 2005). In the case of gravity modelling, background of 2.75 g/cm^3 was used and the Deccan Trap body switched off. Cross-sections are shown in figures 15 to 18. Topography was constructed after the middle cross-section, due to this A-A' and C-C' are shown as not to fit the topography in figures 15 and 17.

Figure 14 depicts the stratigraphical model produced in a plan view. Thus, the model was constructed of three 2.5D polygonal prism bodies. These bodies represent the lake sediments (Body 1), breccia lens (Body 2) and Deccan Trap basalts (Body 3). Shape of the bodies was based on GPS height data which accompanied the TMI measurements, GSI drillhole data, estimates for the thickness of the breccia lens and the Deccan basalts by various authors (Fudali et al. 1980, Subbarao 1994 & 1999, Rajasekhar & Misra 2005, unpublished work by S.S. Rao as cited in Maloof et al. 2010). Body 1, with a side length of 1200 m, was constructed as a lens with a maximum thickness at the crater centre being 100 m. Below it is body 2, with a side length of 1830 m, has a thickness of up to 350 m. Under it is body 3, a rectangle shaped body with an infinite side length, extending further 500 m down.

MODEL PARAMETERS

For the model the following International Geomagnetic Reference Field values were used: field intensity F = 43723 nT, declination D = -0.24°, inclination I = 29°. Susceptibility of the background was set to 0 in the program. The parameters needed for magnetic anomaly modelling for the bodies are *k*, Q, remanent magnetization intensity, declination and inclination. Overview of parameters chosen is shown in Table 3.

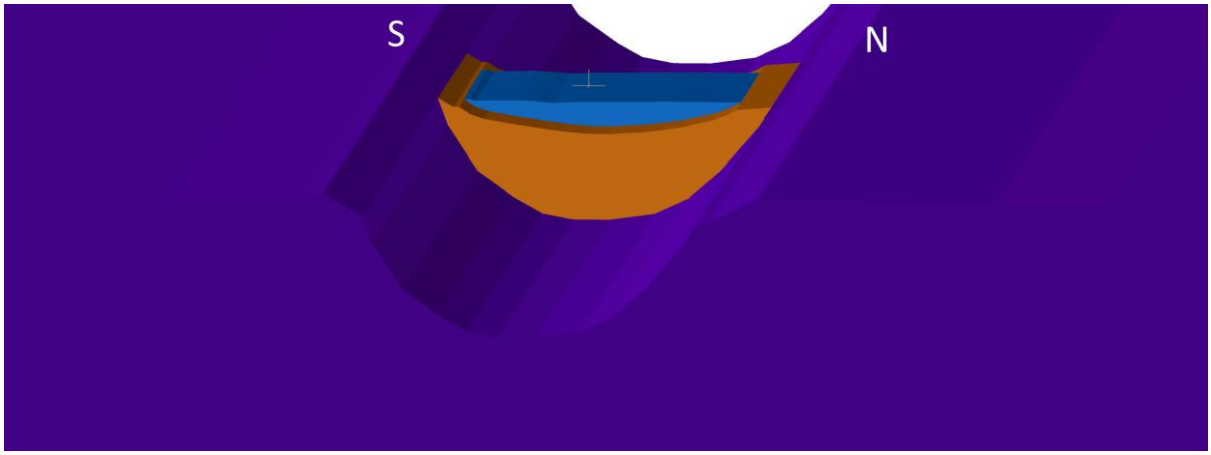

Figure 14. View of the constructed model. Blue lens is the lake sediments, orange lens the breccia and purple the Deccan Trap basalts.

For body 1, the magnetic susceptibility of 6000 $\times 10^{-6}$SI was chosen. Lake sediments consist of relatively high *k* basaltic sand and low *k* silt. To account for the component of sand, a value close to the max *k* value of silty sediments was chosen. Without any data of the remanence for the sediments, Q of 1 was chosen. The crater has a young age, thus natural remanent magnetization (NRM) inclination and declination close to the present day (declination -0.24°, inclination 29°) was preferred. A combination of 0° declination and 10° inclination provided

the best fit for the model. During the modelling process a density of 2.2 g/cm^3 was selected for the lake sediments.

Body 2 was given a *k* of 24000 × 10^{-6}SI. This is the average measured on the basalt flows in the crater wall, during this study. There is no data on the *k* of the breccia itself. It was chosen due to the average obtained in this study is almost half of average measured by Agarwal et al. (2016) and elsewhere for Deccan Trap (Chandrasekhar et al. 2002). The NRM characteristics of breccia must be different from the Deccan Trap basalts. During brecciation, the pieces of rock get moved and oriented randomly, so do their remanence directions, negating the original NRM. Remanence is also already affected by pressures of about 0.5 GPa - 1 GPa (Cisowski and Fuller 1978; Hargraves and Perkins 1969), decline of which was noted in experiments by Nishioka and Funaki (2008) on Lonar basaltic rocks as well. Remanence parameters (declination 0°, inclination 30°) close to the present-day field were applied as NRM for the body. It also fits the model well. The remanence intensity of 0.63 A/m was obtained during the modelling process as the best fit for the final model. This makes the Q value 0.75. Density of 2.72 fit the breccia lens best for the model.

Table 2. Magnetic field parameters found in the literature.

	Natural remanent magnetization		
	Declination (°)	Inclination (°)	Intensity (A/m)
Deccan Traps Primary component (HC/HT)			
Lonar (Vandamme et al. 1991)	157.6	47.4	
Jalna (Rao and Bhalla 1984)	165	44	
Aurangabad (Rao and Bhalla 1984)	149	56	
Rajkot (Chandrasekhar et al. 2002)	141	42	0.32 – 2.72
Saurashtra (Chandrasekhar et al. 2002)	147	56	
Lonar (Louzada et al. 2008)	137.9	55.4	Average intensity - 4.07 (2.38 - 5.28)
Lonar (Rao and Bhalla 1984)	110	61	Average intensity - 4.7
Lonar (Cisowski and Fuller 1978)			Average intensity - 4.8 (1.5 - 12.8)
Deccan Traps Secondary component (LC/LT)			
Lonar background flows (Louzada et al. 2008)	7	30.7	
Lonar (Rao and Bhalla 1984)	9	47	

Body 3 has the most data available on its magnetic properties. Magnetic susceptibility of the Deccan Traps basalts measured by Agarwal et al. (2016) away from the crater have higher *k* values compared to the *k* measured in the current study in the crater and Chandrasekhar et al. (2002) measured an average of 55000 × 10^{-6}SI at Saurashtra. Average of measured values,

40000×10^{-6}SI, by Agarwal et al. (2016) was chosen as a good representation for body 3. Table 2 shows the NRM parameters which are extensively measured at Lonar. Remanent magnetization intensity measurement averages are between 4.07 - 4.8 A/m. Value 4.31 A/m was chosen, making Q = 3.1. Declination and inclination measured at Lonar basalts range from 110 to 157.6° and 42 to 61°, respectively. Values of 132° (declination) and 33° (inclination) fit the model best. The inclination used is close to the measured minimum and can be accepted.

Table 3. Parameters of the bodies used in modelling. Q - königsberger ratio; *k* - magnetic susceptibility; NRM - natural remanent magnetization.

Body	Density(g/cm^3)	Magnetic susceptibility (10^{-6}SI)	Koenigsberger ratio (-)	Natural Remanent Magnetization		
				Intensity (A/m)	Declination (°)	Inclination (°)
Lake sediments (1)	2.2	6000	1	0.21	0	10
Breccia lens (2)	2.72	24000	0.75	0.63	0	30
Deccan Trap (3)		40000	3.1	4.31	132	33

CROSS-SECTIONS

Cross-section locations are depicted in Figure 10. As a result of the modelling, a close match to the observed anomaly is obtained. Figures 15 to 17 show the magnetic anomaly S-N cross-sections and figure 18 the gravity cross-section. The software allows to make cross-sections out of only measured values. Cross-section line in the software is drawn with an assigned width, in this case, 25 m, creating a rectangle which encompasses certain measurement points. These measurement points are used by the software to construct the cross-sections. At the inner rim walls, few measurements could be done due to harsh terrain. For this reason, corresponding areas on the cross-sections are drawn with long straight lines. In reality, they are smoother.

Cross-section A-A' has a slight inconsistency with the observed anomaly. This is seen at the southern rim area, where much higher values are modelled than observed. Aside from this, the model fits well. Removing the effects of the Deccan Trap, a breccia and lake sediment positive anomaly of 250 nT is seen at the southern rim with the anomaly decreasing gradually north to -250 nT at the northern side of the lake. Suddenly values drop to -1400 nT. This is might be a boundary effect of the model, but high negative values are observed there as well. This

magnetic anomaly configuration is consistent with present-day magnetic field directions which should generate a S-N positive to negative gradient.

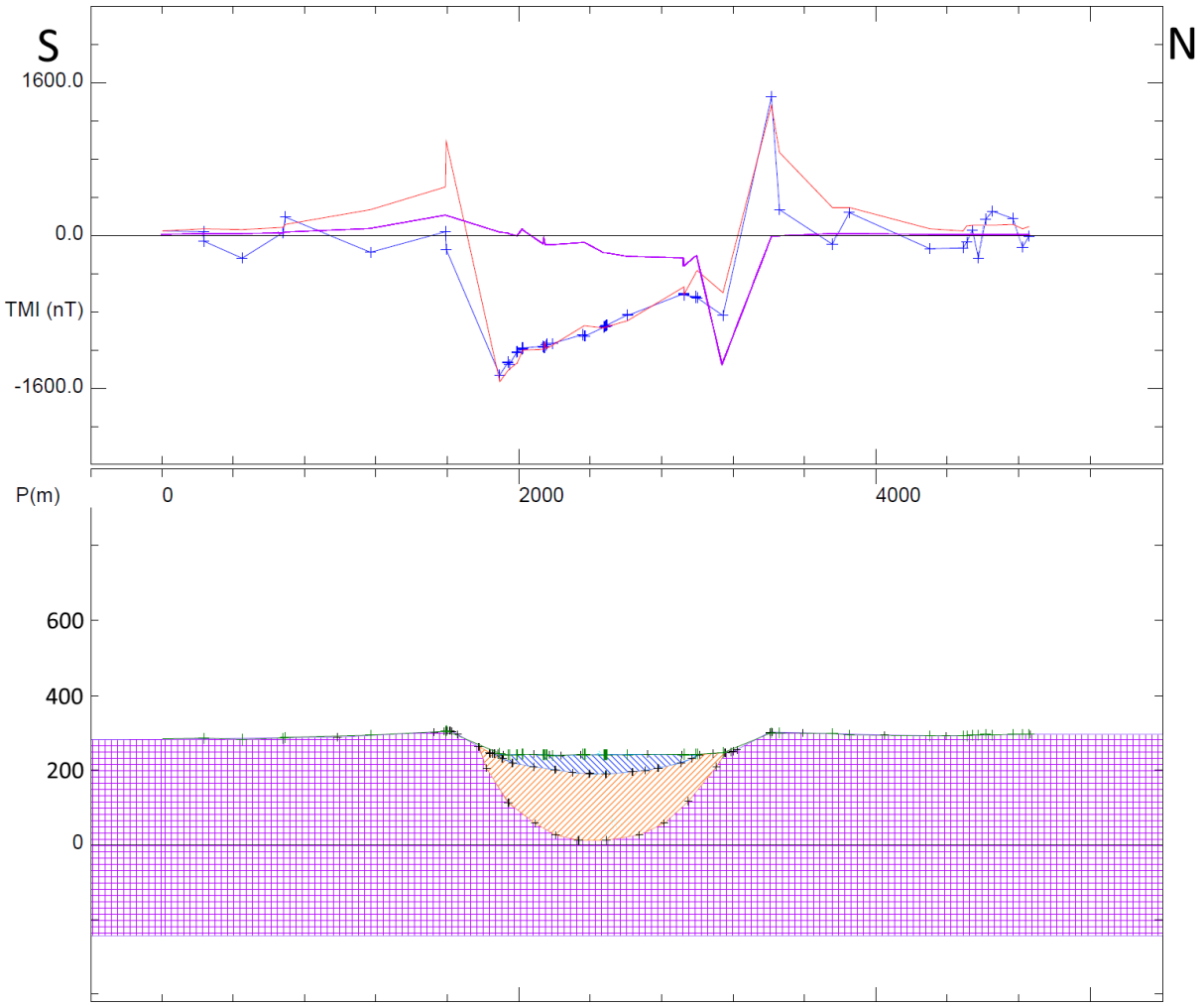

Figure 15. Magnetic profiles and model along the profile A-A' (see Figure 11 for location). Depicting the observed anomaly (blue line with measuring points as blue crosses) and red line as the response created by the model below. Purple line is the magnetic anomaly produced by only lake sediments and breccia. Body 1 (lake sediments) is the blue striped lens, body 2 (breccia) is the yellow striped lens, and body 3 (Deccan Trap basalt) is the purple. Green line at the top of the bodies shows measured topography.

B-B' is the middle cross-section. It produces the closest match to the observed field, which is logical due to the model being constructed after topography of this section. Biggest deviation from the observed field happens at the northern lake shore, where model values turn positive before observed field. After removing the effects of the Deccan Trap, a positive anomaly of about 300 nT is seen at the southern lakeside which decreases smoothly to approximately -400 nT at the northern lakeside.

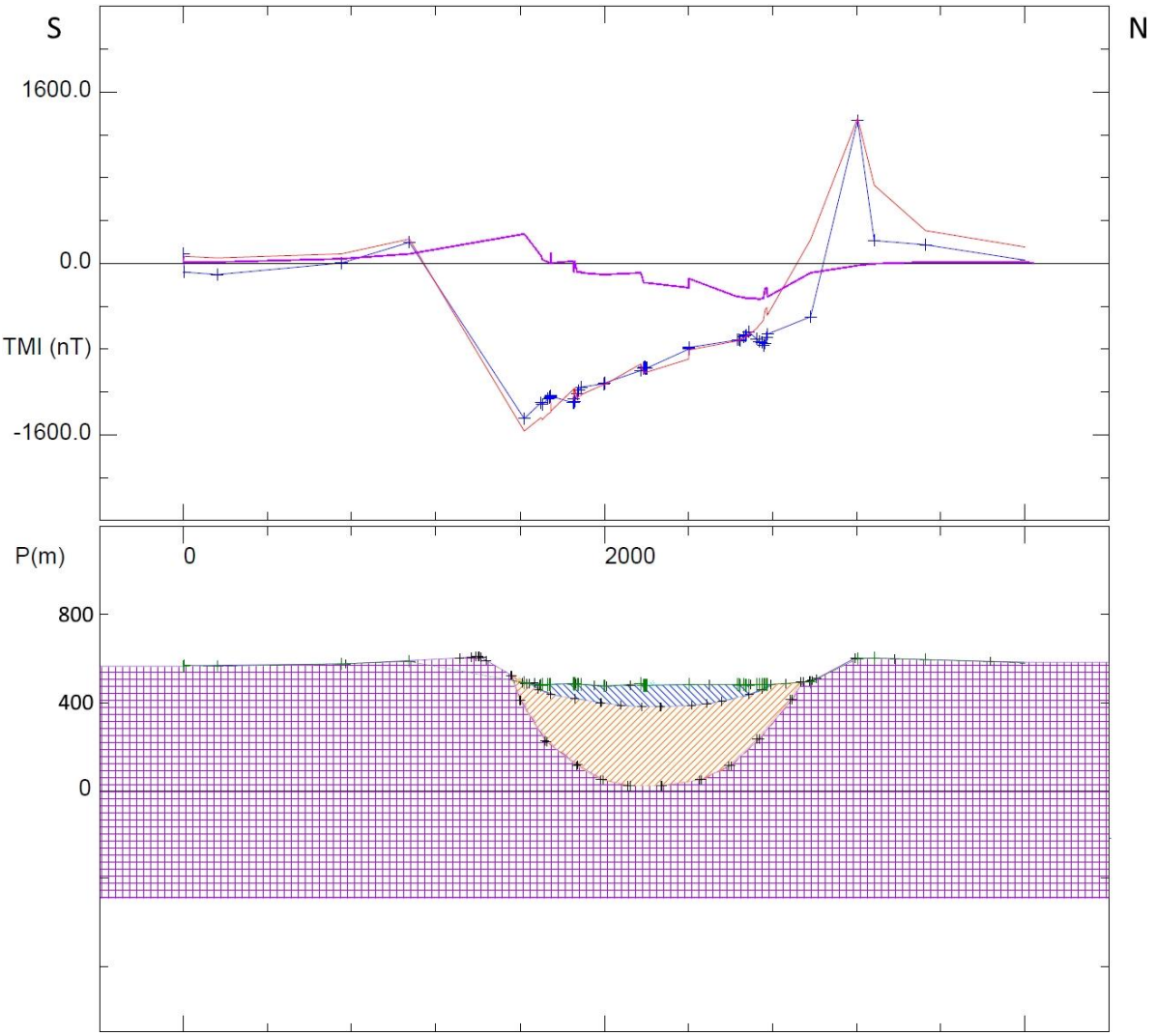

Figure 16. Magnetic profiles and model along the profile B-B' (see Figure 11 for location). Depicting the observed anomaly (blue line with measuring points as blue crosses) and red line as the response created by the model below. Purple line is the magnetic anomaly produced by only lake sediments and breccia. Body 1 (lake sediments) is the blue striped lens, body 2 (breccia) is the yellow striped lens, body 3 (Deccan Trap basalt) is the purple. Green line at the top of the bodies shows measured topography.

Cross-section C-C' has an inconsistency with the measured values at the southern rim, where positive anomalous values of 1600 nT are produced, while the observed field remains at close to 0 nT. Apart from this, it simulates the residual field relatively well. Removing effects of Deccan Trap, a positive anomaly of about 300 nT is seen at the southern lakeside with a smooth decrease toward the N to around -150 nT after which a steep decline to -1200 nT at the northern lakeside. This is similar to the cross-section A-A'.

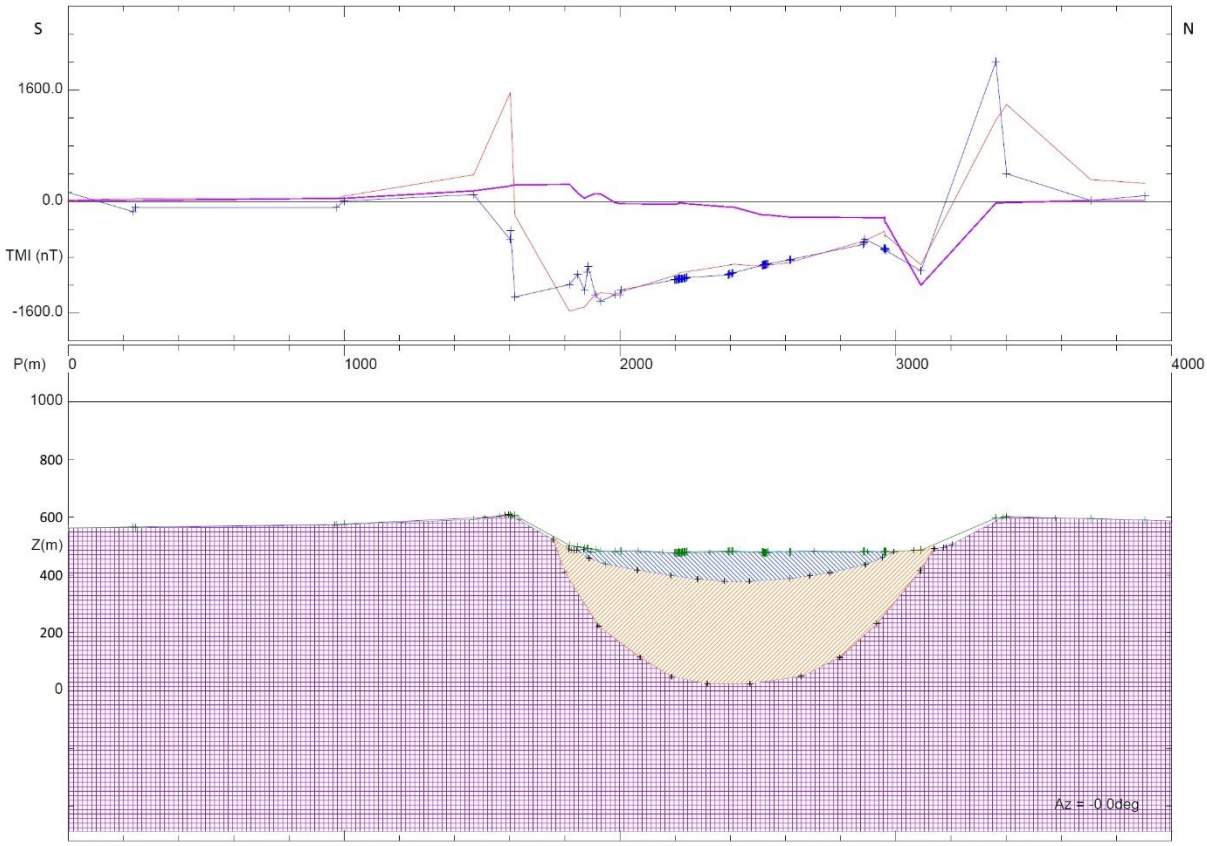

Figure 17. Magnetic profiles and model along the profile C-C' (see Figure 11 for location). Depicting the observed anomaly (blue line with measuring points as blue crosses) and red line as the response created by the model below. Purple line is the magnetic anomaly produced by only lake sediments and breccia. Body 1 (lake sediments) is the blue striped lens, body 2 (breccia) is the yellow striped lens, body 3 (Deccan Trap basalt) is the purple. Green line at the top of the bodies shows measured topography.

The models are most reliable in their centre, where measurements are abundant. At the rim areas the sudden transition between bodies can create anomalies. From cross-sections it is evident that the breccia and lake sediments produce a fraction of the observed field with the Deccan Traps composing a vast part of it.

For the gravity profile G-G' a bowl-shaped anomaly with maximum negative values of 2.25 mGal is modelled. With similar density values (2.2 g/cm^3 for lake sediments, 2.72 g/cm^3 for breccia and 2.75 g/cm^3 for background) to previous researchers this model produces the same gravity anomaly as measured by Fudali et al. (1980).

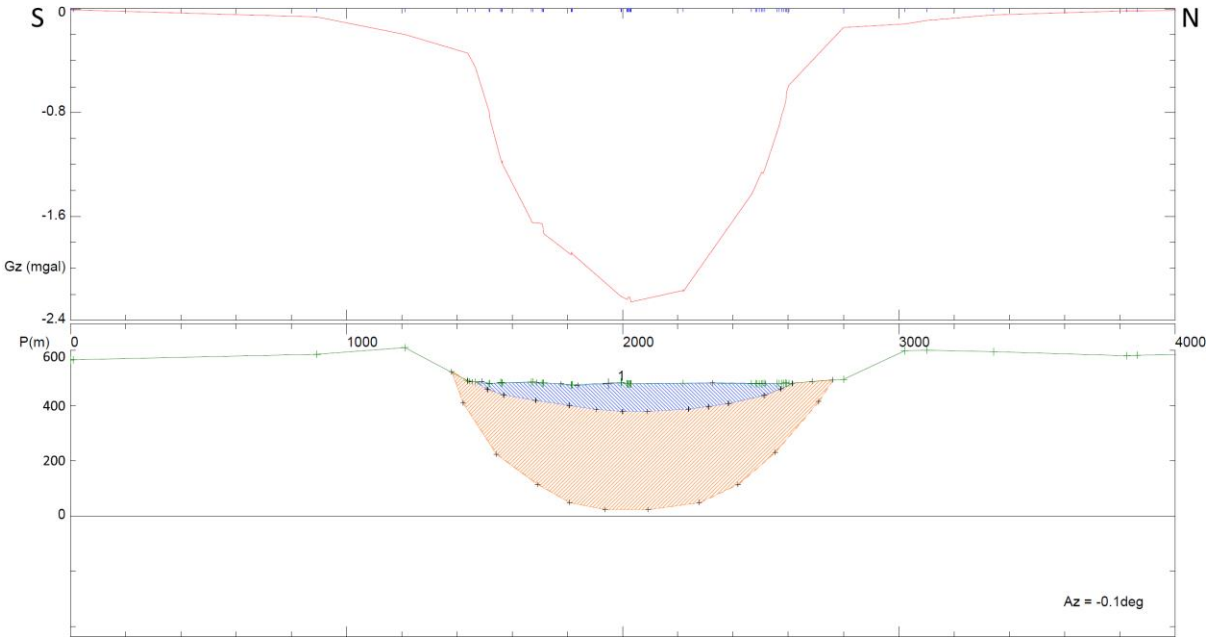

Figure 18. Gravity profile and model along G-G' (see Figure 11 for location). Depicting the modelled gravity anomaly as a red line. Body 1 (lake sediments) is the blue striped lens, body 2 (breccia) is the yellow striped lens. Green line is the measured topography.

4. DISCUSSION

4.1. TOPOGRAPHIC EFFECT OF THE DECCAN TRAP BASALTS

Topographic effects on magnetic data is not a new phenomenon. It has been talked about as early as 1970-s, regarding ocean floor measurements (Parker and Huestis 1974). By nature, an anomaly appears when a magnetic intensity or susceptibility contrast exists. This is caused by a difference between rock formations or a topographical feature such as a deep valley facilitating a rock-air contrast. Additional effect occurs from inclined magnetic field interaction with slopes (Ugalde and Morris 2008). In case of Lonar crater The Deccan Traps have a strong remanent intensity and a high susceptibility with the strength of the magnetic field being three times greater than the Earth's magnetic field. In contrast the lake sediments, breccia, and air, which fill the true crater are magnetized to a lesser degree. For this reason, the Deccan traps generate most of the residual field of the crater and the estimation of the true crater configuration becomes paramount in describing the magnetic anomaly of the breccia.

Estimation of negative and positive landform topographical effects on magnetic data is important. Left unaccounted for interpretations may be geologically erroneous and might obscure the magnetic signal for geological bodies of interest. This is demonstrated for positive landforms by Smekalova and Bevan (2002) and negative landforms by Ugalde and Morris

(2008). If the topographical effect was not assessed in case of Lonar crater, interpretation of the residual field would have required a highly magnetized breccia to exist.

4.2. PREVIOUS MAGNETIC AND GRAVITY FIELD MEASUREMENTS

Unfortunately, the report of Kailasam et al. (1964) is unpublished and could not be obtained. Regardless, description of their measurement absolute values is somewhat comparable to the residual field seen in this study. They explained it by sub-Trap topography and the strong remanent magnetization of basalts with no mention of an impact crater. This explanation is partly correct, because the strong magnetization of Deccan Traps does play a role, but the topographical effect should be considered from the surface to the true crater floor. In addition, the influence of breccia as well as lake sediment low magnetization play a major role in explaining the magnetic anomaly.

Rajasekhar and Mishra (2005) have proposed a gravity and magnetic anomaly model (Figure 4). Their magnetic model is based on vertical component measurements, which show a positive anomaly at the crater centre. They describe it as a product of remagnetization in the present-day Earth's magnetic field after the impact and this anomaly configuration to be caused by induced magnetization. In order to account for this positive anomaly, they modelled a high susceptibility dyke inside the breccia. In stark contrast, our study of TMI measurements show a negative anomaly on the crater floor with no need of a high magnetic susceptibility body to explain the magnetic anomaly observed. This suggests the breccia is rather uniformly magnetized in the direction of the present-day field, while magnetization is much weaker than the surrounding Deccan Traps. The inducing field of the Earth plays a small role due to the surrounding Trap generating a remanent magnetization 3.1 times (Q = 3.1) the strength of the Earth. It is evident that in the case of highly magnetized background, assigning only *k* values, leads to false interpretations.

Removing the Deccan Trap part of the magnetic anomaly a south-north gradient in the magnetic field anomaly is generated by the breccia and lake sediments. Positive values at the southern lakeside are in the range of 300 – 400 nT, reducing to near zero at the crater centre and decrease further to -400 nT at the northern lakeshore. On two of the three (A-A' and C-C') cross-sections a further sudden decrease to -1200 to -1400 nT is observed, which turns back to zero at the rim. These extreme negative values might be a cause of border/edge effect of the model and not entirely trustworthy. A magnetic field anomaly of impact craters is variable but

an anomaly in amplitude of 800 nT is already high and if we believe the extreme negative values, an anomaly in amplitude up to 1800 nT could exist.

Modelled gravity anomaly of Rajasekhar and Mishra (2005) had lake sediments with a density of 2.0 g/cm^3, breccia lens was separated into 2.6 and 2.7 g/cm^3 while the background was set to 2.75 g/cm^3. With these parameters a negative anomaly of -2.25 mGal was modelled in the crater centre just as observed. Our model only corroborates these findings although the lake sediments and breccia lens were given slightly higher densities of 2.2 g/cm^3 and 2.72 g/cm^3.

4.3. MAGNETIC SUSCEPTIBILITY

The magnetic susceptibility of Deccan Trap basalts is variable, having values from 10000 - 80000 μSI (Table 1). Rao and Bhalla (1984) measured magnetic parameters at Lonar and suggested that systematic variations exist in the magnetic intensity, Koenigsberger ratio and magnetic susceptibility. Susceptibility is said to increase from the edges toward the centre of the crater. This is not observed in this study as the *k* values remain variable from the edge toward the centre.

4.4. SHOCK PRESSURE ESTIMATES

Two differing opinions of the shock pressures at Lonar crater exist. Shock pressures affected the magnetic rock magnetic properties on the rim as well as beyond to the west of the crater (Arif et al. 2012; Misra et al. 2010; Nishioka and Funaki 2008). Shock pressure was too low or lasted for such a small duration that the magnetic properties were not affected at the rim (Agarwal et al. 2016; Louzada et al. 2008; Sangode et al. 2017). Model produced in this study supports the idea that the pressures reaching the rim were weak or lasted for a short duration and did not affect magnetic properties of basalts there. Were this not the case, rim with magnetic properties close to Deccan Traps in the model would not characterize the magnetic anomaly so effectively.

4.5. Size of the breccia lens

Initially it was though drilling of the breccia lens in the 1970-s penetrated it (Fredriksson et al. 1973) but that idea was already rejected by Fudali et al. (1980). The deepest drillhole reached 400 m and bottomed in basaltic powder. The nature of the breccia is quite complicated with large blocks of breccia, meters in size, separated by meters of powder. The model created here reaches deeper (450 m for breccia bottom) than the drillholes at Lonar. Rajasekhar and Mishra

(2005) also suggested the depth to the true crater to be more, at a maximum of 500 m. It is likely the drillholes have not penetrated the true extent of the breccia lens.

CONCLUSIONS

Conclusions from model and observations are as follows:

1. The breccia and lake sediments are less magnetized than surrounding Deccan Trap basalts.
2. Breccia has a low uniform NRM most likely due to chaotic pattern of individual vectors.
3. Measured anomaly over Lonar crater is controlled mainly by the topographical effect generated by highly magnetized Deccan Trap basalts.
4. Breccia and lake sediments together generate an estimated magnetic anomaly close to 800 nT in amplitude.
5. Shock pressures at the rim of the crater were not strong enough to affect magnetic properties of basalts to be measurable by ground magnetic mapping.
6. Magnetic susceptibility of Lonar basalts is variable but shows no definitive trends.
7. Drilling done at Lonar by GSI likely did not penetrate the true crater bottom.

In summary, the magnetic method is effective in providing information regarding aspects of the cratering process. At Lonar impact crater, a relatively unique crater in basaltic rocks is especially important because findings there can perhaps be applied to extraterrestrial environments like the Moon or Mars.

KOKKUVÕTE JA JÄRELDUSED

Käesoleva magistritöö objektiks oli Lonar meteoriidikraater. Magistritöö eesmärgiks oli varasemate uurijate Rajasekhar ja Mishra (2005) poolt tehtud magnetvälja mudel ning üldine huvi plahvatusstruktuuridest basaltsetes kivimites, Nendele küsimustele vastamiseks viidi läbi sealse magnetvälja tugevuse ja kivimite magnetilise vastuvõtlikkuse mõõtmised. Magnetvälja tugevust mõõdeti 36 km^2 suurusel alal, mille tulemusena avastati magnetiline anomaalia suurusega -2350 nT kuni 2600 nT. Kõrged väärtused asetsesid vastavalt kraatri lõuna ning põhja vallil. Kraatri põhjas asetses negatiivne anomaalia -1400 nT kuni -400 nT, mille väärtused vähenesid sujuvalt lõunast põhja suunas. Lisaks viidi läbi 203 magnetilise vastuvõtlikkuse mõõtmist kraatri basaltidel (11000 – 65000·10^{-6}SI), järvesetetel (700 – 7900·10^{-6}SI) kui ka väljapaiskematerjalil (2000 – 11000·10^{-6}SI). Mõõdetud informatsiooni kasutati kraatri magnetanomaalia modelleerimisel.

Järeldused mõõtmistest ja modelleerimisest on järgmised:

1. Bretša ning järvesetted on Deccan Trapi basaltidega võrreldes vähem magnetiseeritud.
2. Bretšal on madal ühtlane naturaalne jääkmagnetiseeritus seonduvalt suundade kaootilisusega.
3. Lonar meteoriidikraatris mõõdetud anomaalia on põhjustatud enamasti kõrgelt magnetiseeritud Deccan Trapi basaltide poolt põhjustatud topograafilisest efektist.
4. Bretša ning järvesetted moodustavad magnetvälja anomaalia amplituudiga 800 nT.
5. Plahvatuse põhjustatud rõhud ei olnud vallil piisavalt tugevad, et mõjutada basaltide magnetilisi omadusi, mis oleks tuvastatavad maapealsete magnetvälja mõõtmistega.
6. Lonar meteoriidikraatri basaltide magnetiline vastuvõtlikkus on varieeruv, kuid ei avalda selget gradienti üheski suunas.
7. India geoloogiateenistuse 1970-ndatel läbi viidud puurimised tõenäoliselt ei läbinud bretša läätse.

Magnetilised mõõtmised on väga hea informatsiooni allikas meteoriidikraatri moodustumise protsessidest arusaamiseks. Lonar meteoriidikraatri puhul võivad need eriti tähtsad olla, kuna tegemist on üsnagi unikaalse kraatriga basaltsetes kivimites. Võimalik, et Lonariga seotud avastused saab üle kanda maavälistele kehadele nagu Kuu või Mars.

ACKNOWLEDGEMENTS

I wish to thank my supervisor, Jüri Plado, who proposed this topic and helped me in various ways. I also extend my sincere thanks to Prof. Muddaramaiah Lingadevaru, Phd. students Hamim Jeelani Syed and Sharat Raj B. from the Central University of Karnataka, India and Mateusz Szyszka from Adam Mickiewicz University, Poland for their help with field work.

REFERENCES

Agarwal, Amar, Agnes Kontny, Deepak C. Srivastava, and Reinhard O. Greiling. 2016. "Shock Pressure Estimates in Target Basalts of a Pristine Crater: A Case Study in the Lonar Crater, India." *Bulletin of the Geological Society of America* 128(1–2):19–28.

Arif, Md, N. Basavaiah, S. Misra, and K. Deenadayalan. 2012. "Variations in Magnetic Properties of Target Basalts with the Direction of Asteroid Impact: Example from Lonar Crater, India." *Meteoritics and Planetary Science* 47(8):1305–23.

Chakrabarti, Ramananda and Asish R. Basu. 2006. "Trace Element and Isotopic Evidence for Archean Basement in the Lonar Crater Impact Breccia, Deccan Volcanic Province." *Earth and Planetary Science Letters* 247(3–4):197–211.

Chandrasekhar, D. V, D. C. Ã. Mishra, G. V. S. Poornachandra Rao, and J. Mallikharjuna Rao. 2002. "Gravity and Magnetic Signatures of Volcanic Plugs Related to Deccan Volcanism in Saurashtra , India and Their Physical and Geochemical Properties." 201:277–92.

Chao, E. C. T. 1968. "Pressure and Temperature Histories of Impact Metamorphosed Rocks—Based on Petrographic Observations." *Shock Metamorphism of Natural Materials* 135–58.

Chenet, A., X. Quidelleur, F. Fluteau, V. Courtillot, and S. Bajpai. 2007. "40K–40Ar Dating of the Main Deccan Large Igneous Province: Further Evidence of KTB Age and Short Duration." *Earth and Planetary Science Letters* 263(1–2):1–15.

Chenet, Anne-Lise, Vincent Courtillot, Frédéric Fluteau, Martine Gérard, Xavier Quidelleur, S. F. R. Khadri, K. V Subbarao, and Thor Thordarson. 2009. "Determination of Rapid Deccan Eruptions across the Cretaceous-Tertiary Boundary Using Paleomagnetic Secular Variation: 2. Constraints from Analysis of Eight New Sections and Synthesis for a 3500-m-Thick Composite Section." *J. Geophys. Res* 114:6103.

Cisowski, S. M. and M. Fuller. 1978. "The Effect of Shock on the Magnetism of Terrestrial Rocks." *Journal of Geophysical Research: Solid Earth* 83(B7):3441–58.

Cotton, Charles A. 1952. "Volcanoes : As Landscape Forms." *SERBIULA (Sistema Librum 2.0).*

Crosta, A. P. and M. A. R. Vasconcelos. 2013. "Update on the Current Knowledge of the Brazilian Impact Craters." *Lunar and Planetary Science Conference* 44:4–5.

Dube, A. and S. Sen Gupta. 1978. *Geological Survey of India, DETAILED INVESTIGATION OF LONAR CRATER BULDANA DISTRICT, MAHARASHTRA.*

Fredriksson, K., A. Dube, D. J. Milton, and M. S. Balasundaram. 1973. "Lonar Lake, India: An Impact Crater in Basalt." *Science* 180(4088):862–64.

Fudali, R. F., D. J. Milton, K. Fredriksson, and A. Dube. 1980. "Morphology of Lonar Crater, India: Comparisons and Implications." *The Moon and the Planets* 23(4):493–515.

Fudali, R. F. and Burra Subrahmanyam. 1983. "Gravity Reconnaissance at Lonar Crater, Maharastra." *Special Publication Series - Geological Survey of India* 2:83–87.

Gilbert, C. K. 1896. "The Origin of Hypotheses, Illustrated by Discussion of a Topographical Problem." *Science* 3:1–13.

Grieve, R. A. F., J. M. Coderre, J. Rupert, J. B. Garvin, J. M. Coderre, and J. Rupert. 1989. "Test of a Geometric Model for the Modification Stage of Simple Impact Crater Development." *Meteoritics* 88(2):83–88.

Gupta, Rahul Das, Anupam Banerjee, Steven Goderis, Philippe Claeys, Frank Vanhaecke, and Ramananda Chakrabarti. 2017. "ScienceDirect Evidence for a Chondritic Impactor , Evaporation-Condensation Effects and Melting of the Precambrian Basement beneath the ' Target ' Deccan Basalts at Lonar Crater , India." *Geochimica et Cosmochimica Acta* 215:51–75.

Hargraves, R. B. and W. E. Perkins. 1969. "Investigations of the Effect of Shock on Natural Remanent Magnetism." *Journal of Geophysical Research* 74(10):2576–89.

Harinarayana, T., B. P. K. Patro, K. Veeraswamy, C. Manoj, K. Naganjaneyulu, D. N. Murthy, and G. Virupakshi. 2007. "Regional Geoelectric Structure beneath Deccan Volcanic Province of the Indian Subcontinent Using Magnetotellurics." 445:66–80.

Jay, Anne. 2016. "Stratigraphy , Structure and Volcanology of the SE Deccan Continental Flood Basalt Province : Implications for Eruptive Extent and Volumes Stratigraphy , Structure and Volcanology of the SE Deccan Continental Flood Basalt Province : Implications for Erupt." (January).

Jourdan, F., F. Moynier, C. Koeberl, and S. Eroglu. 2011. "40Ar/39Ar Age of the Lonar Crater and Consequence for the Geochronology of Planetary Impacts." *Geology* 39(7):671–74.

Kailasam, L. N., D. Gupta Sarma, Y. R. Bhanumurth, and P. C. Das. 1964. *Research Report (Unpublished)*.

Komatsu, Goro, P. Senthil Kumar, Kazuhisa Goto, Yasuhito Sekine, Chaitanya Giri, and Takafumi Matsui. 2013. "Drainage Systems of Lonar Crater, India: Contributions to Lonar Lake Hydrology and Crater Degradation." *Planetary and Space Science* 95:45–55.

Lafond, Eugene C. and Robert S. Dietz. 1964. "Lonar Crater, India, a Meteorite Crater?" *Meteoritics* 2(2):111–16.

Lowrie, William and Robert E. Sheriff. 2007. "Fundamentals of Applied Geophysics."

Louzada, Karin L, Benjamin P. Weiss, Adam C. Maloof, Sarah T. Stewart, Nicholas L. Swanson-hysell, and S. Adam Soule. 2008. "Paleomagnetism of Lonar Impact Crater , India." *Earth and Planetary Science Letters* 275(3–4):308–19.

Maloof, Adam C., Sarah T. Stewart, Benjamin P. Weiss, Samuel A. Soule, Nicholas L. Swanson-Hysell, Karin L. Louzada, Ian Garrick-Bethell, and Pascale M. Poussart. 2010. "Geology of Lonar Crater, India." *Bulletin of the Geological Society of America* 122(1–2):109–26.

Masaitis, V. L. 1999. "Impact Structures of Northeastern Eurasia: The Territories of Russia and Adjacent Countries." *Meteoritics and Planetary Science* 34(5):691–711.

Melosh, H. J. 1989. "H. J. Melosh 1989. Impact Cratering. A Geologic Process. Oxford Monographs on Geology and Geophysics Series No. 11. Ix + 245 Pp. Oxford: Clarendon Press. Price £45.00 (Hard Covers). ISBN 0 19 504284 0." *Geological Magazine* 126(06):729.

Melosh, H. Jay. 2004. “Impact Cratering.” Pp. 222–75 in *Planetary Surface Processes*. Cambridge: Cambridge University Press.

Misra, Saumitra, Md Arif, Nathani Basavaiah, P. K. Srivastava, and Anand Dube. 2010. “Structural and Anisotropy of Magnetic Susceptibility (AMS) Evidence for Oblique Impact on Terrestrial Basalt Flows: Lonar Crater, India.” *Bulletin of the Geological Society of America* 122(3–4):563–74.

Misra, Saumitra, Horton E. Newsom, M. Shyam Prasad, John W. Geissman, Anand Dube, and Debashish Sengupta. 2009. “Geochemical Identification of Impactor for Lonar Crater, India.” *Meteoritics and Planetary Science* 44(7):1001–18.

Nakamura, Atsunori, Yusuke Yokoyama, Yasuhito Sekine, Kazuhisa Goto, Goro Komatsu, P. Senthil Kumar, Hiroyuki Matsuzaki, Ichiro Kaneoka, and Takafumi Matsui. 2014. “Formation and Geomorphologic History of the Lonar Impact Crater Deduced from in Situ Cosmogenic 10 Be and 26 Al.” *Geochemistry, Geophysics, Geosystems* 15(8):3190–97.

Nandy, N. and V. Deo. 1961. “Origin of the Lonar Lake and Its Alkalinity.” *TISCO* 8:144–55.

Nishioka, I. and M. Funaki. 2008. “Irreversible Changes in Anisotropy of Magnetic Susceptibility: Study of Basalt from Lonar Crater and Experimentally Impacted Basaltic Andesite.” *Meteoritics and Planetary Science Supplement*.

Pande, K. 2002. “Age and Duration of the Deccan Traps, India: A Review of Radimetric and Paleomagnetic Constraints.” *Proceedings of the Indian Academy of Sciences (Earth Planetary Sciences)* 111(2):115–23.

Philpotts, Anthony and Jay Ague. 2009. *Principles of Igneous and Metamorphic Petrology*. Cambridge: Cambridge University Press.

Pilkington, M. and R. A. F. Grieve. 1992. “The Geophysical Signature of Terrestrial Impact Craters.” *Reviews of Geophysics* 30(2):161–81.

Rajasekhar, Rudravaram Phani and D. Mishra. 2005. “Analysis of Gravity and Magnetic Anomalies over Lonar Lake, India: An Impact Crater in a Basalt Province.” (88):1836–40.

Rao, G. V. S. Poornachandra and M. S. Bhalla. 1984. “Lonar Lake : Palaeomagnetic Evidence of Shock Origin.” 847–62.

Reddy, D. V., T. Madhav, P. Chandrakala, and P. Nagabhushanam. 2015. “A Perspective of Alkaline Lonar Lake, Maharashtra, India with Reference to Its Hydrochemistry.” *Current Science* 109(5):965–75.

Reznik, Boris, Agnes Kontny, and Jörg Fritz. 2017. “Effect of Moderate Shock Waves on Magnetic Susceptibility and Microstructure of a Magnetite-Bearing Ore.” *Meteoritics and Planetary Science* 52(7):1495–1504.

Sangode, S. J., Rajiv Sharma, Rasika Mahajan, N. Basavaiah, Priyeshu Srivastava, Swapnil S. Gudadhe, D. C. Meshram, and M. Venkateshwarulu. 2017. “Anisotropy of Magnetic Susceptibility and Rock Magnetic Applications in the Deccan Volcanic Province Based on Some Case Studies.” *Journal of the Geological Society of India* 89(6):631–42.

Sengupta, D. and N. Bhandari. 1988. “Formation Age of the Lonar Crater.” *Abstracts of Papers Submitted to the Lunar and Planetary Science Conference, Vol.19, Part 3* (May):1059–60.

Sengupta, D., N. Bhandari, and S. Watanabe. 1997. “Formation Age of Lonar Meteor Crater, Indi.” *Revista de Fisica Aplicada e Instrumentacao* 12(December):1–7.

Smekalova, Tatiana N. and Bruce W. Bevan. 2002. “The Magnetic Anomaly of a Mound.” (December).

Subbarao, K. V. 1999. “Deccan Volcanic Province: Memoir 43(1 and 2).” *Geological Society of India, Bangalore*.

Subrahmanyam, Burra. 1985. “Lonar Crater, India: A Crypto-Volcanic Origin.” *Geological Society of India* 26(5).

Ugalde, Hernan and Bill Morris. 2008. “An Assessment of Topographic Effects on Airborne and Ground Magnetic Data.” *The Leading Edge* 27(1):76–79.

Wadia, D. .. 1919. *Geology of India for Students*. London.

Weiss, Benjamin P., Shelsea Pedersen, Ian Garrick-Bethell, Sarah T. Stewart, Karin L. Louzada, Adam C. Maloof, and Nicholas L. Swanson-Hysell. 2010. “Paleomagnetism of Impact Spherules from Lonar Crater, India and a Test for Impact-Generated Fields.” *Earth and Planetary Science Letters* 298(1–2):66–76.

ZH Instruments. 2009. *Magnetic Susceptibility Meter USER ’ S MANUAL*. Czech Republic.

APPENDIX 1.

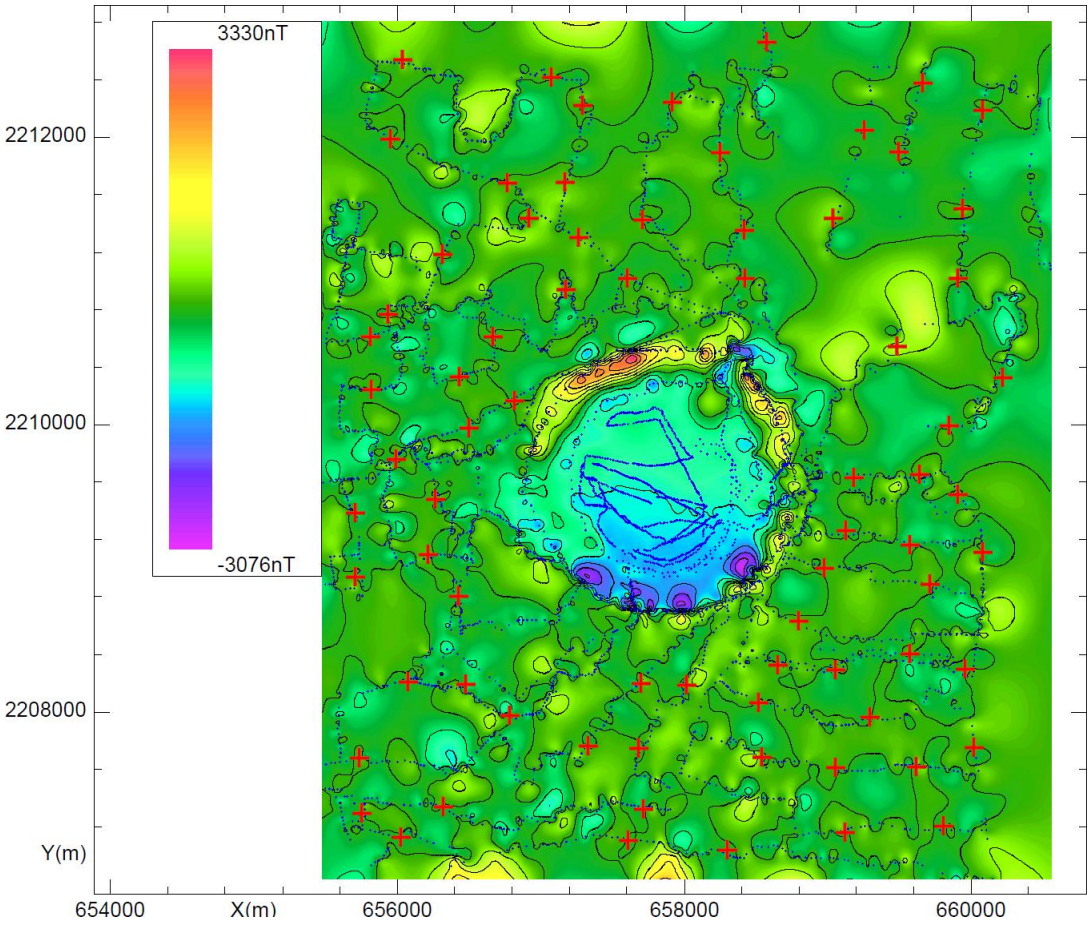

Control points (red crosses) used for regional field removal.

Non-exclusive licence to reproduce thesis and make thesis public

I, Kalle Kiik

herewith grant the University of Tartu a free permit (non-exclusive licence) to

1. reproduce, for the purpose of preservation, including for adding to the DSpace digital archives until the expiry of the term of copyright,

Magnetic anomaly model of the Lonar meteorite impact crater in Maharastra, India

supervised by Jüri Plado,

2. I grant the University of Tartu a permit to make the work specified in p. 1 available to the public via the web environment of the University of Tartu, including via the DSpace digital archives, under the Creative Commons licence CC BY NC ND 3.0, which allows, by giving appropriate credit to the author, to reproduce, distribute the work and communicate it to the public, and prohibits the creation of derivative works and any commercial use of the work until the expiry of the term of copyright.

3. I am aware of the fact that the author retains the rights specified in p. 1 and 2.

4. I certify that granting the non-exclusive licence does not infringe other persons' intellectual property rights or rights arising from the personal data protection legislation.

Kalle Kiik

03/06/2019